1   **Dissection of the corticotroph transcriptome in a mouse model of**

2   **glucocorticoid-induced suppression of the HPA axis**

3   Romanò N[1], Duncan PJ[1], McClafferty H[1], Nolan O[1], Ding Q[1], Homer NZ[2], Le Tissier

4   P[1], Walker BR[2,3], Shipston MJ[1], Chambers TJG[1,4].

5

6   1. Centre for Discovery Brain Sciences, Hugh Robson Building, 15 George

7   Square, University of Edinburgh, Edinburgh, EH8 9XD, UK

8   2. Centre for Cardiovascular Science, Queen's Medical Research Institute, 47

9   Little France Crescent, Edinburgh EH16 4TJ

10 3. Translational & Clinical Research Institute, Newcastle University, Newcastle

11   upon Tyne, NE1 7RU

12 4. Edinburgh Centre for Endocrinology and Diabetes, Royal Infirmary of

13   Edinburgh, Little France, Edinburgh EH16 4SA

14

15 Corresponding author: tom.chambers@ed.ac.uk

16

17 Word count: 6316

18

19 Key words: Chronic, Glucocorticoid, Recovery, HPA axis

20   **ABSTRACT**

21   Glucocorticoids (GC) are prescribed for periods >3 months to 1-3% of the UK

22   population; 10-50% of these patients develop hypothalamus- pituitary-adrenal (HPA)

23   axis suppression, which may last over 6 months and is associated with morbidity and

24   mortality. Recovery of higher nodes of the axis is necessary for recovery of adrenal

25   function. We developed a mouse model of Dexamethasone (DEX)-induced HPA axis

26   dysfunction in order to further explore recovery in the pituitary. Adult male C57BL6/J

27   or those crossed with *Pomc*-eGFP mice were randomly assigned to receive DEX

28   (~0.4 mg/kg bodyweight/day) or vehicle via drinking water for 4 weeks following

29   which treatment was withdrawn. Tissues were harvested at 0, 1, and 4 weeks

30   following withdrawal of treatment. Corticotrophs were isolated from *Pomc*-eGFP

31   pituitaries using FACS, and RNA extracted for RNA-seq. DEX treatment suppressed

32   corticosterone production, which remained partially suppressed at least 1 week

33   following DEX withdrawal. In the adrenal, at time 0, *Hsd3b2, Cyp11a1*, and *Mc2r*

34   mRNA levels were significantly reduced, with *Mc2r* and *Cyp11a1* remaining reduced

35   1 week following DEX withdrawal. The corticotroph transcriptome was modified by

36   DEX treatment with some differences between groups persisting 4 weeks following

37   withdrawal. No genes supressed by DEX exhibited ongoing attenuation 1 and 4

38   weeks following withdrawal, whilst only 2 genes were upregulated and remained so

39   following withdrawal. A pattern of rebound at 1 and 4 weeks was observed in 14

40   genes that increased following suppression, and 6 genes that were reduced by DEX

41   and then increased. Chronic GC treatment may induce persistent changes in the

42   pituitary that may influence future response to GC treatment or stress.

43   **INTRODUCTION**

44   Since the observation of the profound effect of administration of Kendall's compound

45   E (Cortisone) on the inflammatory condition rheumatoid arthritis (Hench *et al.* 1949),

46   glucocorticoids (GCs) have become a principal treatment for inflammatory conditions

47   across most body systems to the extent that they are now prescribed to 1-3% of the

48   adult population (Fardet *et al.* 2011; Bénard-Laribière *et al.* 2017; Laugesen *et al.*

49   2017). Despite the evolution of steroid-sparing treatments, prescription rates

50   continue to increase each year (Fardet *et al.* 2011; Laugesen *et al.* 2017).

51   Exogenous GCs suppress endogenous GC production. When treatment is stopped,

52   homeostasis should re-activate the HPA axis; however, this does not always occur,

53   sometimes with fatal consequences (Fraser *et al.* 1952). Failure of GC production

54   following withdrawal of chronic (>3 month) GC treatment is common (30-50% of

55   people immediately after stopping treatment, 10-20% of people 6 months later

56   (Broersen *et al.* 2015; Joseph *et al.* 2016)). Such cases likely have a significant

57   clinical impact; there is a 2-3x increase in hospital presentations with symptoms and

58   signs of adrenal insufficiency (hypotension, hypovolaemia, cardiovascular collapse,

59   and hypoglycaemia) in the 4 week period following discontinuation of chronic

60   systemic GC treatment (Laugesen *et al.* 2019).

61   We are unable to accurately identify those patients at most clinical risk; meta-

62   analyses suggest that age, dose, and cumulative dose are likely predictors

63   (Broersen *et al.* 2015; Joseph *et al.* 2016; Laugesen *et al.* 2019) although these only

64   account for some of the variability observed between patients. We also currently

65   have no means of predicting recovery of the HPA axis at the point of starting GC

66   therapy, and thus cannot tailor expensive and involved testing or increased use of

67   steroid-sparing agents to those most at risk of adrenal insufficiency following

68   withdrawal. Certainly, there would be huge clinical benefits to both improve

69   identification of those most at risk and the rate of recovery in those with a

70   suppressed axis.

71   Chronic GC treatment suppresses all levels of the HPA axis. For example, there are

72   blunted adrenocorticotrophic hormone (ACTH) and cortisol responses to insulin-

73   induced hypoglycaemia (Schlaghecke *et al.* 1992); impaired reactivity of the pituitary

74   to CRH testing (Schürmeyer *et al.* 1985; Schlaghecke *et al.* 1992) and an impaired

75   reactivity of the adrenal to ACTH1-24 (Borresen *et al.* 2017). Importantly, the

76   recovery of ACTH production is essential for recovery of adrenal activity in patients

77   both following treatment for Cushing's disease and in patients where treatment with

78   supra-physiological exogenous GCs is withdrawn (Graber *et al.* 1965). During

79   recovery there is marked increase in ACTH above physiological levels that precedes

80   recovery of adrenal function.

81   We established a mouse model to understand the recovery process of the HPA axis

82   following withdrawal of chronic GC treatment. Recovery of the pituitary corticotroph

83   population following withdrawal of chronic GC is essential for recovery of the HPA

84   axis (Graber *et al.* 1965; Hodges & Sadow 1969; Nicholson *et al.* 1984). Having

85   found evidence for disrupted corticotroph function persisting up to one week

86   following withdrawal of GC, and given *in vitro* evidence for long term (120h)

87   transcriptional changes as a result of only a brief (24h) GC exposure (Jubb *et al.*

88   2017), we hypothesised that chronic GC exposure would program sustained

89   changes in the corticotroph transcriptome. We reasoned that persistent changes to

90   transcriptional regulators or to pathways regulating ACTH synthesis and secretion

91   might explain the delay in corticotroph and thus HPA axis recovery.

92 **RESULTS**

93 Mice were analysed in 4 groups: those exposed to only drinking water (control;

94 Group A), exposed to dexamethasone (DEX) for 4 weeks (Group B), exposed to

95 DEX for 4 weeks and then switched to drinking water for 1 week (1 week recovery,

96 Group C) or exposed to DEX for 4 weeks and then switched to drinking water for 4

97 weeks (4 week recovery, Group D)(Figure 1).

98 *Body and adrenal weight*

99 Weight gain was attenuated during treatment with DEX. Upon discontinuation of

100 DEX (in group B), weight increased over 28 days to match that of control litter mates.

101 There was a significant interaction between weight, time, and treatment $p < 0.001$

102 (Figure S1A). Adrenal weight was reduced following treatment and 1 and 4 weeks

103 following withdrawal but this failed to reach the threshold considered significant of

104 $p < 0.05$ (Fig. 2A and 2B and S1B). In experiments 1 and 3, when adrenals were

105 collected at the start of the rest period, this difference remained evident 4 weeks

106 after stopping the DEX. Adrenal/bodyweight ratio was not significantly affected by

107 DEX or withdrawal (Figure 2C and D).

108 *Steroid levels*

109 Corticosterone levels were significantly reduced by DEX treatment (Fig. 2E and F).

110 When tested at waking – peak corticosterone levels – this finding persisted even 1

111 week after stopping the DEX (Figure 2 F). 11-Dehydrocorticosterone levels were

112 also reduced by DEX but in both waking and resting phases had recovered 1 week

113 after stopping the DEX (Figure 2G and H). ACTH levels were lower immediately after

114 stopping DEX, though this did not achieve statistical significance. One week after

115 stopping the DEX, two distinct populations of animals were apparent: those with

116   increased ACTH levels (indicating recovery of the higher HPA axis (dotted box)) and

117   those with lower levels than would be expected given the relatively low

118   corticosterone levels (dashed box) (Figure 2F). Two mice had ACTH levels and

119   corticosterone levels consistent with controls (blue circles) (normal corticosterone

120   and low ACTH). This is further exemplified in Figure 2F where the animals in group B

121   (1 week following recovery) form into disparate groups; low ACTH and low

122   corticosterone (dashed box- ongoing HPA axis suppression), high ACTH and low

123   corticosterone (dotted box, recovered pituitary, ongoing adrenal suppression), and

124   normalised ACTH and corticosterone (recovered). DEX levels measured in the

125   plasma from experiment 2 were not detectable in the control group (A) or in group C

126   or D, 1 and 4 weeks after treatment withdrawal, highlighting this was not the reason

127   for lower corticosterone levels in group C. Among those animals exposed to DEX

128   (Group B), plasma DEX levels reached maximally 6nM (Figure S1C).

129   *Adrenal and hypothalamic gene expression*

130   In experiment 1, DEX treatment had no impact on mRNA detected for *Avp, Crh,*

131   Glucocorticoid receptor (*Nr3c1*), or Mineralocorticoid receptor *(Nr3c2)* in whole

132   hypothalamus (Fig. 3A).

133   Gene expression was examined in the adrenal glands from experiments 1 (rest

134   period) and 2 (wake period). DEX treatment significantly reduced expression of

135   mRNA for the ACTH receptor (*Mc2r*), the steroidogenic enzymes *Cyp11a1* (side

136   chain cleavage enzyme) and *Hsd3b2* (3-beta hydroxylase), the first two steps in the

137   steroidogenic pathway, *Star* the gene coding the steroid acute regulatory protein,

138   and the gene coding *Mrap*, which transports the ACTH receptor to the plasma

139   membrane. One week following DEX withdrawal, there was ongoing reduced

140   expression of *Mc2r*, *Mrap*, *Cyp11a1*, and *Star* mRNA. The reduction in mRNA for

141   these genes was greatest in the pm/wake period when, in control animals (group A)

142   corticosterone levels were the highest. Thus, changes to mRNA were present in the

143   adrenal which persist at least one week after withdrawing DEX treatment, consistent

144   with the lower corticosterone levels measured at waking in this group. mRNA levels

145   of the glucocorticoid and mineralocorticoid receptors were significantly increased as

146   a result of DEX treatment, remaining significantly elevated even four weeks after

147   DEX withdrawal in the case of the mineralocorticoid receptor (*Nr3c2*).

148   *Pituitary gene expression*

149   In humans, following withdrawal of supraphysiological GC, the recovery of adrenal

150   responsiveness to ACTH follows recovery of pituitary ACTH production (presumably

151   a result of the trophic effect of ACTH on the adrenal). In fact, there tends to be an

152   overshoot in ACTH production (as would be seen in primary adrenal failure) prior to

153   recovery of the adrenal (Graber *et al.* 1965). Sustained changes to transcription of

154   the GC responsive gene *Fkbp5* persisting 120h beyond GC withdrawal have been

155   found *in vitro* (Jubb *et al.* 2017). We wished to explore whether transcriptional

156   dynamics were persistently affected following DEX withdrawal and might associate

157   with HPA axis dysfunction. We took advantage of the *Pomc*-eGFP transgenic mouse

158   line to isolate *Pomc* expressing cells from the anterior pituitary in order to assess the

159   corticotroph transcriptome during DEX treatment and following treatment withdrawal

160   (experiment 3). Pilot studies showed ongoing suppression of *Pomc* mRNA in isolated

161   corticotrophs 1 week following DEX withdrawal. We were interested in identifying if

162   other genes showed sustained changes following withdrawal of DEX .

163   The eGFP expression as measured at the time of FACS exhibited in general a bi-

164   modal distribution, suggesting the existence of two sub-populations of *Pomc*

165   expressing cells sorted from the anterior pituitary (Fig. 4A). DEX induced a shift of

166   cells to the lower eGFP-expressing population, which was most apparent four weeks

167   after DEX withdrawal.

168   Treatment with DEX had no impact on the abundance of isolated cells (Fig.S2C),

169   although it did induce a small but not statistically significant reduction in the

170   proportion of GFP-positive cells. RNA-seq confirmed a reduction in *Pomc* mRNA in

171   response to DEX (Fig 4C). Interestingly, 1 week following treatment withdrawal

172   (Group C; green), there was variability in *Pomc* mRNA with increased *Pomc* mRNA

173   in 2 pools, but the third pool had returned to control levels (Figure 4B and 4D).

174   Of a total of 23,247 genes (with >0.1 read/million in>3 samples), 151 were

175   differentially expressed between the four groups (using cut off false discovery rate

176   <0.05). Primary component analysis showed that control, DEX treatment, and 4-

177   week recovery animals roughly clustered together (Fig 4C) but Group C were

178   dispersed by both PC1 and PC2. The 60 genes exhibiting the most significant

179   difference between groups are shown in Figure 4B. Interestingly all four groups had

180   a distinct transcriptomic signature, particularly remarkable for group D despite this

181   group showing recovery of the HPA axis by measurement of steroidogenesis. DEX

182   treatment resulted in 63 significantly up- and 12 significantly down-regulated genes

183   (log2 fold change >2).

184   We were next interested in genes that showed persistent changes. We used our

185   dataset of 151 significantly changed genes (FDR <0.05) to find genes that showed

186   persistent changes with log2 fold change of 1 vs. controls (group A). Only small

187   groups of genes showed a persistent change in expression as a result of DEX

188   exposure. 1 gene (*Igha*) was suppressed by DEX and was also suppressed 1 week

189   after treatment withdrawal and 8 genes were both upregulated by DEX and remained

190   elevated one week after withdrawal (*Plb1 Krt19 Fbn1, Ido1, Penk, Klk1b24, Oaf*, and

191   *Col8a2)* two of these remained increased four weeks DEX post withdrawal (*Plb1* and

192   *Krt19*) (Table 1). The majority of differentially expressed genes were increased by

193   DEX and then returned to normal (73 genes) at 1 and 4 weeks.

194   Another pattern of 'rebound' expression was observed, group 4 and group 3 in Table

195   1. These groups may represent genes that were directly or indirectly stimulated or

196   repressed by GC. 17 genes were upregulated by DEX and then suppressed at 1 or 4

197   weeks, and 6 genes were upregulated by DEX and then suppressed.

198   Ontological analysis using Protein Analysis Through Evolutionary Relationships,

199   http://pantherdb.org (Mi *et al.* 2019) identified transporter activity (e.g. GO:0005215;

200   GO:0015075) and kinase activity (GO:0016301) as the molecular processes most

201   affected by DEX (Table 2). Dividing these genes into those up- or down-regulated by

202   DEX further highlighted some classes of molecular function of importance: genes

203   with peptidase/ hydrolase were enriched in those down-regulated by DEX, in

204   particular a number of Kalikrein genes, along with the transporters identified above

205   (Supplemental table 1). Of those suppressed by DEX, antigen binding, extra cellular

206   matrix components, and G-protein coupled receptors were significant (Supplemental

207   table 2).

208   A further analysis examining the molecular function of pathways that were changed

209   across all groups is shown in Table 2. Here, pathways that were identified as

210   significantly up- or down-regulated in comparisons between control and each of the

211   three treatment groups are shown. For example, G protein-coupled receptor activity

212   (GO:0004930) was down-regulated by DEX but showed a rebound increase. Cation

213   transmembrane transporter activity (GO:0008324) on the other hand was up-

214   regulated by DEX and then reduced during the recovery period.

215   We assessed differentially expressed gene sets for regulator regions using I-cis

216   (Imrichová *et al.* 2015). Consistent with induction by GC, we found enrichment for

217   genes associated with binding sites for *Nr3c1* (the glucocorticoid receptor)

218   (normalised enrichment score 5.48, >3 deemed significant). A stronger association

219   was identified between H3K27me3, a marker of heterochromatin (NES 13.8), and

220   those genes up-regulated in our model by chronic DEX treatment. Interestingly, we

221   did not find enrichment for GR in the genes suppressed by DEX, this might be as the

222   algorithm is less effective at identifying the distal enhancers associated with DEX

223   suppression (McDowell *et al.* 2018). Instead, we found enrichment for CHD2 (a

224   chromatin helicase), and H3K36me3 (which usually marks gene bodies, but can also

225   be found in heterochromatin) (NES 12.1 and 11.8, respectively).

METHODS

Studies were performed according to the Animals (Scientific Procedures) Act 1986 following specific approval from the UK Home Office (Project Licence P09E1F821), following review by the University of Edinburgh Animal Research Ethics Committee and in compliance with EU directive 2010/63/EU. Data are presented from three experiments (Figure 1). Experiments 1 and 2 used male 8-week-old C57Bl6/J mice (Jackson Laboratories, UK). Experiment 3 used *Pomc*-eGFP (Pinto *et al.* 2004) transgenic mice maintained on a C57Bl6/J background and bred in-house. Mice were acclimatised to controlled lighting conditions in the animal facility for two weeks prior to each experiment, at constant temperature (22°C). Animals were fed standard chow supplemented with sunflower seeds.

Experiment 1

Mice (C57Bl6/J, n = 36) were housed 6 per cage with lights on 07:00-19:00, and then randomly assigned to receive dexamethasone (DEX) (~0.4 mg/kg/day)(Sigma Aldrich, UK) in drinking water, or vehicle for 4 weeks (Figure 1A). This dose of DEX would be the allosteric equivalent of 2.5 mg for a 70 kg human, the equivalent to around 16 mg of prednisolone. This 'moderate' dose sits in the middle of the range of a weaning dose of 40 mg down to 5 mg over 8-12 weeks commonly used to treat flares of rheumatoid arthritis or inflammatory bowel disease. Animals were weighed three times per week. Following 4 weeks treatment, DEX was withdrawn and animals were maintained in standard conditions thereafter. At withdrawal of DEX (time = 0), one week and four weeks, six animals per group, selected randomly, 2 per cage were sacrificed by cervical dislocation between 9 and 11am (early rest period). Whole pituitary, hypothalamus, and adrenal glands were dissected and frozen on dry ice and then stored at -80°C. Adrenal glands were weighed. Trunk

251   blood was obtained and serum separated by centrifugation at 2000 *x g* for 10

252   minutes at 4°C and stored at -20°C. Glucose was measured using an Accuchek

253   Aviva glucometer (Roche, UK).

254   *Experiment 2*

255   Mice (C57Bl6/J, n = 48) were randomly assigned to four groups and were housed 3

256   animals per cage: Group A (control) received drinking water for 8 weeks; Group B (0

257   weeks recovery) received standard drinking water for 4 weeks and then DEX for 4

258   weeks; Group C (1 week recovery) received standard drinking water for 3 weeks,

259   then DEX for 4 weeks with a final week of recovery; Group D (4 weeks recovery)

260   receiving DEX in drinking water as above for four weeks with a switch to standard

261   water for the following four weeks (Figure 1B). Two weeks prior to the start of the

262   experiment lighting was reversed (lights on 21:00, lights off 09:00), otherwise

263   conditions were as experiment 1. At the end of the experiment mice were randomly

264   assigned to receive 30 minutes of restraint stress 20-60 minutes prior to sacrifice. As

265   there was no significant effect of stress on measurements taken, these two groups

266   have been combined. Mice were sacrificed by cervical dislocation and trunk blood

267   collected into cold tubes prepared with 5 μL of 5% EDTA and placed on ice. Plasma

268   was obtained by centrifugation as above and stored at -80°C until analysis. Anterior

269   pituitary, hypothalamus, and adrenal were dissected and frozen on dry ice and

270   stored at -80°C. All animals were sacrificed between 9:40 and 11:45 am (early wake

271   period).

272   *Experiment 3*

273   *Pomc*-eGFP mice (n = 36) were randomly assigned to the four groups described in

274   experiment 2, three animals per cage with lights on 07:00-19:00 (Figure 1C). At the

275   end of the experimental protocol, mice were sacrificed by cervical dislocation

276   between 9:35 and 10:30am (early rest period). Plasma, hypothalamus, adrenal, and

277   pituitaries were harvested as above. The posterior and intermediate pituitary lobes

278   were carefully dissected and anterior pituitaries were dissociated as previously

279   (Duncan *et al.* 2015). The early time point was chosen here to fit with other models

280   being established in our laboratory. Briefly, pooled tissues, each pool from three

281   mice, were minced with a razor blade before being placed into 2.5 ml DMEM with 25

282   mM Hepes (LifeTechnologies) supplemented with 10 μl/ml DNAse I (Sigma) and

283   0.25% trypsin (Worthington). The pituitaries were digested for 20 minutes at 37°C

284   with gentle shaking every 5 minutes. Digestion was terminated by allowing cells to

285   settle, removing the supernatant and trituration of the cells in 1 ml DMEM

286   supplemented with 50 μl soybean trypsin inhibitor (Sigma), 50 μl Aprotinin (100

287   Kallikrein units) (Sigma), and 5 μl DNAse I. Cells were passed through a 70 μm cell

288   strainer that was washed with further inhibition solution. Cells were then centrifuged

289   10 minutes at 100g at room temperature, the supernatant was removed and the cells

290   resuspended in DMEM supplemented with 4.5 g/l glucose with L-glutamine and 25

291   mM HEPES (Life technologies), 0.3% BSA, 1x ITS liquid media supplement (Sigma),

292   4.2 µg/ml fibronectin (Sigma), and 1x antibiotic/antimycotic solution (Sigma)

293   (penicillin, streptomycin, and amphotericin B) and triturated gently before being

294   transported to the FACS facility.

295

296   *Isolation of eGFP positive cells*

297   Cells were resuspended in 500 μl PBS supplemented with 25 mM HEPES and 5 mM

298   EDTA (FACS buffer) and passed through a 35 μm cell strainer that was washed with

299   a further 200 μl of the FACS buffer. Draq7 was added as a vitality marker and cells

300   sorted using a Sony SH800. Gates were established using WT pituitaries to avoid

301   capturing eGFP negative ve cells and to select single cells. Sorted single cells were

302   resuspended into low bind Eppendorf tubes into 300 μl Trizol and were frozen on dry

303   ice and stored at -80°C until sending for sequencing.

304   *RNA Extraction, QC, Library Preparation, and Illumina Sequencing*

305   RNA isolation, library preparation, and sequencing reactions were conducted at

306   GENEWIZ, LLC. (South Plainfield, NJ, USA). Total RNA was extracted from FACS

307   sorted cells using Qiagen RNeasy Plus Universal Mini kit followed by manufacturer's

308   instructions (Qiagen, Hilden, Germany). The RNA samples were quantified using

309   Qubit 2.0 Fluorometer (Life Technologies, Carlsbad, CA, USA) and were below the

310   limit of detection.

311   Ultra-low input RNA sequencing library preparation used the Clontech SMART-V4 kit

312   for cDNA Synthesis from 10 pg-10 ng total RNA and polyA amplification. Illumina

313   Nextera XT kit was used to prepare the final DNA libraries according to

314   manufacturer's instructions. Integrity of the sequencing library was assessed on the

315   Agilent TapeStation (Agilent Technologies, Palo Alto, CA, USA), and quantified by

316   using Qubit 2.0 Fluorometer (Invitrogen, Carlsbad, CA) as well as by quantitative

317   PCR (KAPA Biosystems, Wilmington, MA, USA).

318   The sequencing libraries were clustered on one lane of a patterned flowcell. After

319   clustering, the flowcell was loaded on the Illumina HiSeq 4000 or equivalent

320   instrument in High Output Mode according to manufacturer's instructions. The

321   samples were sequenced using a 2x150 Paired End (PE) configuration. Image

322   analysis and base calling were conducted by the HiSeq Control Software (HCS).

323   Raw sequence data (.bcl files) generated from Illumina HiSeq were converted into

324   fastq files and de-multiplexed using Illumina's bcl2fastq 2.17 software. One

325   mismatch was allowed for index sequence identification.

326   *Steroid quantification*

327   For experiment 1, 11-dehydrocorticosterone (A) and corticosterone (B) were

328   measured by tandem liquid chromatography mass spectrometry (LC-MS/MS) in 30

329   μL of serum at the mass spectrometry core facility, University of Edinburgh. Briefly,

330   plasma (30 μL) was enriched with internal standards (D4-cortisol (D4F) and epi-

331   corticosterone ((Epi-B), 2.5 ng). Chloroform (10:1) was added and vortexed. The

332   supernatant was reduced to dryness under oxygen-free nitrogen (OFN) at 60°C and

333   reconstituted in water:acetonitrile(70 μL; 70:30 (v/v)). Samples were extracted

334   alongside a calibration curve of A and B with D4F and epi-B as internal standards.

335   Quantitative analysis of the extracts was carried out on a Shimadzu Nexera – Sciex

336   QTrap 6500+ LC-MS/MS instrument, operated in positive ion mode, as described

337   previously (Nixon *et al.* 2016; Verma *et al.* 2019).

338   For experiment 2, a low volume automated extraction method was developed for

339   mouse plasma and combined with an LC-MS/MS method adapted from (Agnew *et al.*

340   2019), to detect corticosterone, 11-dehydrocorticosterone, and dexamethasone by

341   LC-MS/MS in only 10 μL of mouse plasma. Briefly, 10 μL of plasma was diluted to

342   100 μL with water, prepared alongside a calibration curve of the steroids of interest.

343   The plasma, calibration standards, and blanks were dispensed manually as aliquots

344   (100 μL) into individual wells of a 2 mL 96 deep-well polypropylene plate (Waters,

345   UK). An internal standard solution of isotopically labelled standards (d8-

346   corticosterone (Cambridge isotope laboratories), and d4-dexamethasone (Sigma-

347   Cerrilliant)) in methanol was added (20 μL; 10 ng) to each well except for the double

348   blanks. The plate was agitated on a plate shaker (2 minutes) and transferred to a

349   Biotage® Extrahera™ automated sample processor (Biotage, Uppsala, Sweden)

350   where formic acid (100 μL, 0.1%, v/v) was added to each well. Samples were

351   incubated at room temperature (18-22°C; 5 minutes) and transferred to an SLE+ 200

352   plate by the robot, loaded onto the SLE material under positive pressure using

353   compressed air. Following a wait (5 minutes) the analytes were eluted from the SLE

354   material into a deep-well collection plate by positive pressure following the addition

355   of dichloromethane/propan-2-ol (98:2; 4x 450 μL). The eluate was dried down under

356   a stream of heated oxygen free nitrogen (OFN, 40°C) on an SPE Dry™ Dual Sample

357   Concentrator System (Biotage, Uppsala, Sweden). Once dry the extracts were

358   dissolved in water/methanol (70:30, 100 μL), the plate was sealed then shaken on a

359   plate shaker (10 minutes) and sealed with a zone-free plate seal, before injecting

360   directly from the 96-well plate for LC-MS/MS analysis.

361   Samples were injected (10 μL) onto a Kinetex C18 column (150 × 3 mm; 2 μm,

362   Phenomenex, Macclesfield, UK) at 40°C using a flow rate of 0.5 mL/min, mobile

363   phase A – water 0.05 mM ammonium fluoride, B – methanol 0.05 mM ammonium

364   fluoride from 55 to 100% B over 16 minutes, protected by a Kinetex KrudKatcher

365   (Phenomenex, Macclesfield, UK), followed by analysis on a QTrap 6500+ Linear Ion

366   Trap Quadrupole Mass Spectrometer (AB Sciex, UK) system TurboIonspray source

367   operated at 600°C. A, B, and dexamethasone were detected with the following

368   transitions; m/z 345.1.1→ 121.2, m/z 347.1 → 121.1, m/z 393.1 → 373.2 while

369   internal standards d8-corticosterone and d4-dexamethasone were detected with the

370   following transitions; m/z 355.3 → 125.1 and m/z 397.1 → 377.2.

371   The peak areas of each steroid and each internal standard were integrated using

372   Quantitate in Analyst 1.6.3. Linear regression analysis of calibration standards,

373   calculated using peak area ratios of steroid of interest to internal standard, was used

374   to determine the concentration of the steroid of interest in the samples. $R_2 > 0.99$

375   was considered acceptable and within each batch of samples the accuracy at the

376   upper and lower limits were only accepted if accuracy <20%. The amount of steroid

377   was calculated using linear regression analysis of the peak area ratio.

378   *ACTH quantification*

379   ACTH was measured in 25 - 50 μl of plasma using an ACTH ELISA kit M046006

380   (MD biosciences, Switzerland) according to manufacturers' instructions. The assay

381   has low cross-reactivity with other products of *Pomc*. Samples were diluted 1:4 or

382   1:8. The assay had a lower limit of detection of 4 pg/ml, has an intra-assay precision

383   (CV) of 6.7% and an inter-assay precision (CV) of 7.1%.

384   *qRT-PCR*

385   RNA was extracted from tissue using the Reliaprep miniprep system (Promega, UK)

386   according to the standard protocol except that treatment with DNase to remove

387   genomic DNA was extended for 30 minutes. RNA purity was assessed using

388   spectrophotometry to ensure 260/280 readings were >1.8. RNA integrity for subsets

389   of samples was assessed by inspection of RNA on a 1% agarose gel. RNA was

390   reverse transcribed using Superscript IV (Thermo-Fisher, UK) in accordance with

391   manufacturer's instructions with random hexamers and oligodT (50:50). qRT-PCR

392   was conducted using an ABI 7500 and relative expression determined, with stably

393   expressed reference genes determined using NormFinder: for experiment 1, adrenal

394   reference genes were *Gapdh* and *Ipo8*; for pituitary, *Ppia* and *Ipo8*; and for

395   hypothalamus, *Ppia* and *Gapdh*. For experiment 2 (adrenal) *Gapdh* and *Fbox10*

396   were used as house keeping genes. Data are presented as delta-delta Ct versus the

397   control; in experiment 1 the control from the same time point and in experiment 2

398   with the control arm (group A).

Statistics

400   Differences between groups were assessed by linear mixed model. Normality was

401   assessed by visualisation of q-q plots. For experiment 1, treatment and time were

402   used as dependent variables and cage as a random variable. For experiments 2 and

403   3, group was used as the dependent variable and cage as a random factor. For

404   assessing bodyweight, group and time were used as dependent variables and

405   individuals within cage as random factors to allow for repeated measures. For ease

406   of comparison of qPCR experiments and quantification of glucocorticoids, data from

407   experiment 1 were further analysed grouping together results from the different times

408   in the control arm (delta Ct still relative to the time point control). Where a significant

409   interaction between time and treatment was identified (experiment 1), or an effect of

410   group (experiment 1, 2, and 3), pairwise comparison was made, corrected for using

411   Tukey's HSD. Statistical analysis was conducted using R version 3.6.2; $p < 0.05$ was

412   taken as statistically significant. Data are referred presented in box and whisker plots

413   (with median and interquartile range).

RNA-seq bioinformatic analysis

415   Nextera adapters were removed from paired end FASTA files using trimgalore v0.6.5

416   using the flags –paired and –2colour. Quality control, including successful removal of

417   adapters, assessment of phred scores and sequence length were assessed using

418   FastQC v0.11.9. Trimmed reads were aligned to the mouse genome (GRCm38

419   release 98) using STAR v2.7.1a. Aligned reads were quantified using featureCounts

420   v2.0.0 using the flags -p (paired end), -Q 20 (mapping quality >20) and -s 2 (reverse

421   stranded) (Liao *et al.* 2014). Count files were then analysed by EdgeR keeping

422   genes with >0.1 counts per million (cpm) in at least three samples and with

423   differential expression based upon trended dispersion. For comparison with qRT-

424   PCR data (Fig. 3C), cpm relative to the control group (A) were calculated for each

425   gene. 17.5 million to 27.1 million reads were obtained from each sample of

426   corticotrophs pooled from three pituitaries (Fig. S2C).

DISCUSSION

We exposed mice to the synthetic GR agonist, DEX for four weeks in drinking water and show sustained suppression of the HPA axis persisting for at least one week following treatment withdrawal. We showed that at one week following DEX withdrawal, some animals show a compensatory increase in plasma ACTH and corticotroph *Pomc* expression whilst others still demonstrate suppressed corticotroph action given the relative corticosterone deficiency. DEX has a significant effect on the corticotroph transcriptome; whilst one week following treatment withdrawal, the majority of genes affected by DEX have returned to control levels, a number of genes do retain differential expression that is persistent at least 1 week after withdrawal of DEX, and which may play a role in disrupted activity.

As expected, we found evidence for reduced adrenal function persisting one week following withdrawal of DEX treatment (Finco *et al.* 2018; Spiga *et al.* 2020). A non-significant but persistent reduction in adrenal size and a significant reduction in the abundance of transcripts for genes regulating steroidogenesis was found one week following DEX withdrawal. Glucocorticoid-producing cells of the zona fasciculata are generated from *Gli1* and *Shh* expressing progenitor cells both in response to stress (Steenblock *et al.* 2018), and recovery from withdrawal of exogenous glucocorticoid treatment (Finco *et al.* 2018). The signals driving adrenal recovery in this paradigm are unclear; whilst ACTH certainly drives hypertrophy of the zona fasciculata (Baccaro *et al.* 2007), other endocrine and paracrine factors (e.g. sympathetic stimulation (Steenblock *et al.* 2018) and VEGF signalling (Mallet *et al.* 2003)) also play a role in driving recovery. In mice, co-treatment with ACTH attenuates DEX-induced adrenal atrophy further, highlighting the trophic role of this hormone in the adrenal (Mallet *et al.* 2003).

452   The adrenal response to ACTH is reduced both in humans and in rodent models

453   following withdrawal of chronic exogenous GC treatment (Borresen *et al.* 2017;

454   Spiga *et al.* 2020). Previous studies highlight normalised ACTH plasma

455   measurements in the context of ongoing adrenal insufficiency, suggesting an

456   ongoing defect at the level of the adrenal (Schuetz *et al.* 2008; Borresen *et al.* 2017;

457   Spiga *et al.* 2020). However, another interpretation of these data is that ACTH levels

458   should be increased in the milieu of relative adrenal insufficiency and thus

459   normalised ACTH levels are suggestive of ongoing attenuated corticotroph (or

460   hypothalamic) function. Further, that expression of the steroidogenic enzymes that

461   remain suppressed one week following DEX withdrawal are driven by ACTH

462   (Ruggiero & Lalli 2016) might also point towards ongoing impaired activity at the

463   higher HPA axis. Taken together, data suggest that exogenous GC exposure

464   suppresses both adrenal and pituitary function, and confirm that recovery of adrenal

465   function is dependent (at least in part) upon recovery of the pituitary.

466   One week following withdrawal of DEX, we find heterogeneity in the HPA axis

467   activity of mice. In the waking phase (pm) we show that whilst 5 of 9 mice exhibit the

468   expected increase in ACTH associated with impaired adrenal function (consistent

469   with recovery of corticotroph activity), 2 of 9 have ACTH that is inappropriately low

470   given the low corticosterone levels. We see a similar pattern in the transcriptome of

471   isolated corticotrophs where 1 pool out of 3 shows low (similar to control) levels of

472   *Pomc* transcript when this should be elevated in the context of adrenal insufficiency.

473   This variability is reminiscent of human studies where only a proportion of patients

474   are found to have ongoing adrenal insufficiency following withdrawal of exogenous

475   GC (e.g. 10% of patients at 6 months) (Dinsen *et al.* 2013; Joseph *et al.* 2016). The

476   data suggest inter-individual differences in the trajectory of recovery of the mice in

477   terms of ACTH release that could be established in further studies looking at further

478   'snap shots' of the recovery process following DEX withdrawal.

479   A number of possibilities could account for these differences: (1) we show variance

480   in the levels of plasma DEX attained as a result of the exposure in drinking water,

481   thus the variability could be attributed to different dose exposures as a result of

482   differences in water intake as mice were co-housed; (2) social hierarchy may affect

483   HPA axis activity as observed in Cynmolgus (Jimenez *et al.* 2017) (although we

484   pooled from a cage each for each experiment); (3) finally, factors that influence GC

485   sensitivity of the HPA axis, for example epigenetic changes in the hypothalamus as a

486   result of early life or prenatal stress exposure (Ostrander *et al.* 2006; van Bodegom

487   *et al.* 2017; Matthews & McGowan 2019), could account for inter-individual

488   differences.

489   DEX at 0.4 mg/kg likely reaches lower concentrations within the blood brain barrier

490   than plasma; 0.2 mg/kg/mouse reached brain concentrations of 30% that of plasma

491   as a result of extrusion by Mdr1/Abcb1 (Schinkel *et al.* 1995), a p-glycoprotein that

492   helps to reduce accumulation of toxins within the brain, and which exports DEX.

493   Thus a relative GC deficient state was likely induced by our DEX exposure. We did

494   not find changes in whole hypothalamus transcript levels for *Crh* or *Avp* when

495   measured in the rest period. The magnocellular component (which does not

496   contribute directly to HPA axis activity) in which these transcripts are also found

497   abundantly may account for the lack of change here. As we have dissected whole

498   hypothalamus we are unable to assess specific changes in the parvocellular

499   neurones that regulate anterior pituitary hormone release.

500   We explored recovery at the level of the pituitary further by isolating corticotrophs

501   from *Pomc*-eGFP mice. The eGFP profile of the isolated cells exhibited a bimodal

502   distribution, most apparent in groups A and C; in groups B and D there was a shift in

503   the population to the left with a greater proportion of 'low eGFP' expressing cells.

504   Two possibilities to account for multiple populations of cells arise here. First,

505   inclusion of melanotrophs that also produce large quantities of *Pomc*. These cells

506   were removed by careful dissection of the *pars intermedia*, but some melanotrophs

507   may be present in the anterior pituitary (Mayran *et al.* 2019). We did not find any

508   association between expression of *Pcsk2* and *Pax7*, markers of melanotrophs, and

509   those samples with larger populations of eGFP 'high' cells. Further our own

510   experience with dispersed GFP +ve cells *in vitro* suggests that <1% of cells fail to

511   respond to CRH/AVP, a mechanism specific to corticotrophs. Given that in some

512   pools of cells, >30% of cells made up those in the eGFP 'high' peak, it is hard to

513   reconcile that these cells all made up melanotrophs of the anterior pituitary.

514   However, we cannot discount the fact that the population may have included some

515   melanotrophs. Second, that corticotroph cells can exist in two 'states'. To date single

516   cell RNA-seq from pituitaries suggests a spectrum of transcriptomic activity (as

517   assessed by levels of *Pomc* transcript) in cells identified as corticotrophs (Cheung *et*

518   *al.* 2018). Variable transcription rates across a population are reminiscent of those

519   described from live cell imaging of pituitary lactotrophs (Featherstone *et al.* 2016).

520   Thus a heterogenous population of corticotroph cells may have been shifted 'left' to

521   form a more homogenous population by treatment with DEX, leaving the possibility

522   that the pituitary has undergone physiological change that has not been detected by

523   basal ACTH and corticosterone measurement.

524   As previous *in vitro* studies had shown a persistent stimulation of *Fkbp5* mRNA

525   expression following withdrawal of DEX (Jubb *et al.* 2017), we wished to assess if

526   the chronic DEX treatment in mice resulted in sustained transcriptional changes in

527   the corticotrophs that might explain the delay in recovery of the HPA axis. Only 1

528   gene was supressed by DEX and exhibited ongoing suppression either 1 or 4 weeks

529   following treatment withdrawal. 2 of the 101 genes up-regulated by DEX remained

530   elevated 4 weeks after withdrawal of the DEX, with 5 genes showing ongoing up-

531   regulation 1 week after DEX withdrawal. We thus found little evidence to support

532   persistent global dysregulation of gene expression as a result of DEX exposure, but

533   we did find a small number of genes with persistent differential expression, at least at

534   1 week after stopping the DEX

535   We identified several genes with differential expression 1 week after withdrawal of

536   DEX that may play a role in regulation of corticotroph activity. Two G-protein-coupled

537   receptors with known significance in corticotroph biology were reduced by DEX

538   exposure, but showed significant increase during the recovery process. *Sstr2*, the

539   somatostatin 2 receptor is a target of Pasireotide, which is being trialled for use in

540   treatment of Cushing's disease. The change in expression of *Sstr2* as a result of GC

541   exposure could have implications for the efficacy of this treatment, and selection of

542   patients most likely to benefit (Lacroix *et al.* 2020). *Aplr*, the apelin receptor is of

543   interest as apelin is a stimulator of ACTH release and steroidogenesis (Newson *et al.*

544   2009; Yang *et al.* 2019). This effect was previously attributed to a paracrine effect

545   within the hypothalamus but these data suggest a direct role on corticotroph function

546   is possible, which may affect signalling even one month following withdrawal of

547   therapy. The transporter *Slc12a5*, (also known as KCC2) was also up-regulated by

548   DEX, the channel is inhibited by loop diuretics, and *in* vitro has been shown to inhibit

549   ACTH release (Heisler 1991). Further transporter/ion channel proteins were

550   identified with hitherto unknown function in corticotrophs. These may make novel

551   targets for limiting ACTH release in patients with Cushing's, but also potential

552   pathways that could be activated to try to increase the rate of recovery in patients

553   with GC-induced adrenal insufficiency or disordered HPA axis regulation. We also

554   identified a collection of kallikrein genes up-regulated by DEX. Previous experiments

555   have shown small reductions in ACTH release in response to hypoglycaemia where

556   rats were co-treated with a kallikrein inhibitor (Madeddu *et al.* 1992); thus, this is a

557   potential mechanism further inhibiting ACTH release in response to GC. A number of

558   genes associated with extra-cellular matrix were identified, *Fbn1, Col3a1*, and

559   *Mfap4*. Given persistent changes seen in some of these genes following DEX

560   withdrawal, it is interesting to postulate that the intercellular network of corticotophs

561   may have been affected by DEX, as has been seen in lactotrophs following 1_{st}

562   lactation (Hodson *et al.* 2012).

563   There are a number of limitations to our study. The number of timepoints we have

564   studied has been limited by resources, and thus we have only looked at a small

565   number of 'snap shots' during the recovery process. The dynamics of recovery

566   between these time points, and if these exhibit inter-individual differences would be

567   important foci for future work. Further, as we required to pool pituitaries in order to

568   obtain sufficient numbers of corticotrophs for RNA-sequencing, our data lack

569   resolution at the individual level. Mice likely experienced stress at time of sacrifice,

570   and whilst procedures were kept consistent for all experiments, perceived stress

571   could account for some of the variation in hormone (especially ACTH)

572   measurements.

573   To conclude, we established a model of chronic glucocorticoid treatment in mice and

574   found that 28 days of DEX exposure had suppressed HPA activity, which persisted 7

575   days following treatment withdrawal. DEX treatment had a persistent effect on

576   adrenal steroidogenesis and abundance of adrenal transcripts for steroidogenic

577   enzymes that lasted at least 7 days. DEX suppressed corticotroph *Pomc*

578   transcription, an effect which had recovered in some animals one week following

579   withdrawal but persisted in others, mirroring the pattern seen in ACTH measurement.

580   Earlier time points during recovery and an increase the number of individuals would

581   be useful for future experiments examining regulation of suppression, and recovery

582   of hypothalamic and corticotroph activity following chronic GC exposure. A persistent

583   but small change in the transcriptome of *Pomc*-expressing isolated GFP positive

584   cells was identified 4 weeks following DEX withdrawal. This was not associated with

585   altered corticosterone or ACTH production, but might affect further pituitary response

586   to other stimuli, for example repeat steroid prescription or stress, and could

587   contribute to the longevity of HPA axis suppression seen in some humans following

588   withdrawal of chronic GC treatment.

REFERENCES

Agnew EJ, Garcia-Burgos A, Richardson RV, Manos H, Thomson AJW, Sooy K, Just G, Homer NZM, Moran CM, Brunton PJ *et al.* 2019 Antenatal dexamethasone treatment transiently alters diastolic function in the mouse fetal heart. *Journal of Endocrinology* **241** 279–292. (doi:10.1530/JOE-18-0666)

Baccaro RBF, Mendonça POR, Torres TEP & Lotfi CFP 2007 Immunohistochemical Jun/Fos protein localization and DNA synthesis in rat adrenal cortex after treatment with ACTH or FGF2. *Cell and Tissue Research* **328** 7–18. (doi:10.1007/s00441-006-0352-8)

Bénard-Laribière A, Pariente A, Pambrun E, Bégaud B, Fardet L & Noize P 2017 Prevalence and prescription patterns of oral glucocorticoids in adults: a retrospective cross-sectional and cohort analysis in France. *BMJ Open* **7** e015905. (doi:10.1136/bmjopen-2017-015905)

van Bodegom M, Homberg JR & Henckens MJAG 2017 Modulation of the Hypothalamic-Pituitary-Adrenal Axis by Early Life Stress Exposure. *Frontiers in Cellular Neuroscience* **11**. (doi:10.3389/fncel.2017.00087)

Borresen SW, Klose M, Baslund B, Rasmussen ÅK, Hilsted L, Friis-Hansen L, Locht H, Hansen A, Hetland ML, Lydolph MC *et al.* 2017 Adrenal insufficiency is seen in more than one-third of patients during ongoing low-dose prednisolone treatment for rheumatoid arthritis. *European Journal of Endocrinology* **177** 287–295. (doi:10.1530/EJE-17-0251)

Broersen LHA, Pereira AM, Jørgensen JOL & Dekkers OM 2015 Adrenal Insufficiency in Corticosteroids Use: Systematic Review and Meta-Analysis. *The Journal of Clinical Endocrinology & Metabolism* **100** 2171–2180. (doi:10.1210/jc.2015-1218)

Cheung LYM, George AS, McGee SR, Daly AZ, Brinkmeier ML, Ellsworth BS & Camper SA 2018 Single-Cell RNA Sequencing Reveals Novel Markers of Male Pituitary Stem Cells and Hormone-Producing Cell Types. *Endocrinology* **159** 3910–3924. (doi:10.1210/en.2018-00750)

Dinsen S, Baslund B, Klose M, Rasmussen AK, Friis-Hansen L, Hilsted L & Feldt-Rasmussen U 2013 Why glucocorticoid withdrawal may sometimes be as dangerous as the treatment itself. *European Journal of Internal Medicine* **24** 714–720. (doi:10.1016/j.ejim.2013.05.014)

Duncan PJ, Şengül S, Tabak J, Ruth P, Bertram R & Shipston MJ 2015 Large conductance Ca^{2+}-activated K^+ (BK) channels promote secretagogue-induced transition from spiking to bursting in murine anterior pituitary corticotrophs. *The Journal of Physiology* **593** 1197–1211. (doi:10.1113/jphysiol.2015.284471)

Fardet L, Petersen I & Nazareth I 2011 Prevalence of long-term oral glucocorticoid prescriptions in the UK over the past 20 years. *Rheumatology* **50** 1982–1990. (doi:10.1093/rheumatology/ker017)

Featherstone K, Hey K, Momiji H, McNamara AV, Patist AL, Woodburn J, Spiller DG, Christian HC, McNeilly AS, Mullins JJ *et al.* 2016 Spatially coordinated dynamic gene transcription in living pituitary tissue. *ELife* **5** e08494. (doi:10.7554/eLife.08494)

Finco I, Lerario AM & Hammer GD 2018 Sonic Hedgehog and WNT Signaling Promote Adrenal Gland Regeneration in Male Mice. *Endocrinology* **159** 579–596. (doi:10.1210/en.2017-03061)

Fraser CG, Preuss FS & Bigford WD 1952 Adrenal atrophy and irreversible shock associated with cortisone therapy. *Journal of the American Medical Association* **149** 1542–1543.

Graber AL, Ney RL, Nicholson WE, Island DP & Liddle GW 1965 NATURAL HISTORY OF PITUITARY-ADRENAL RECOVERY FOLLOWING LONG-TERM SUPPRESSION WITH CORTICOSTEROIDS. *The Journal of Clinical Endocrinology and Metabolism* **25** 11–16. (doi:10.1210/jcem-25-1-11)

Heisler S 1991 ACTH secretion from mouse pituitary tumor cells is inhibited by loop diuretic drugs. *European Journal of Pharmacology* **208** 131–136. (doi:10.1016/0922-4106(91)90063-n)

Hench PS, Kendall EC, Slocumb CH & Polley HF 1949 Adrenocortical Hormone in Arthritis *. *Annals of the Rheumatic Diseases* **8** 97–104.

Hodges JR & Sadow J 1969 Hypothalamo-pituitary-adrenal function in the rat after prolonged treatment with Cortisol. *British Journal of Pharmacology* **36** 489–495. (doi:10.1111/j.1476-5381.1969.tb08005.x)

Hodson DJ, Schaeffer M, Romanò N, Fontanaud P, Lafont C, Birkenstock J, Molino F, Christian H, Lockey J, Carmignac D *et al.* 2012 Existence of long-lasting experience-dependent plasticity in endocrine cell networks. *Nature Communications* **3** 605. (doi:10.1038/ncomms1612)

Imrichová H, Hulselmans G, Kalender Atak Z, Potier D & Aerts S 2015 i-cisTarget 2015 update: generalized cis-regulatory enrichment analysis in human, mouse and fly. *Nucleic Acids Research* **43** W57–W64. (doi:10.1093/nar/gkv395)

Jimenez VA, Allen DC, McClintick MN & Grant KA 2017 Social Setting, Social Rank and HPA Axis Response in Cynomolgus Monkeys. *Psychopharmacology* **234** 1881–1889. (doi:10.1007/s00213-017-4596-7)

Joseph RM, Hunter AL, Ray DW & Dixon WG 2016 Systemic glucocorticoid therapy and adrenal insufficiency in adults: A systematic review. *Seminars in Arthritis and Rheumatism* **46** 133–141. (doi:10.1016/j.semarthrit.2016.03.001)

Jubb AW, Boyle S, Hume DA & Bickmore WA 2017 Glucocorticoid Receptor Binding Induces Rapid and Prolonged Large-Scale Chromatin Decompaction at Multiple Target Loci. *Cell Reports* **21** 3022–3031. (doi:10.1016/j.celrep.2017.11.053)

663   Lacroix A, Bronstein MD, Schopohl J, Delibasi T, Salvatori R, Li Y, Barkan A, Suzaki N,
664   Tauchmanova L, Ortmann C-E *et al.* 2020 Long-acting pasireotide improves clinical
665   signs and quality of life in Cushing's disease: results from a phase III study. *Journal of*
666   *Endocrinological Investigation*. (doi:10.1007/s40618-020-01246-0)

667   Laugesen K, Jørgensen JOL, Sørensen HT & Petersen I 2017 Systemic glucocorticoid use in
668   Denmark: a population-based prevalence study. *BMJ Open* **7** e015237.
669   (doi:10.1136/bmjopen-2016-015237)

670   Laugesen K, Petersen I, Sørensen HT & Jørgensen JOL 2019 Clinical indicators of adrenal
671   insufficiency following discontinuation of oral glucocorticoid therapy: A Danish
672   population-based self-controlled case series analysis. *PLOS ONE* **14** e0212259.
673   (doi:10.1371/journal.pone.0212259)

674   Liao Y, Smyth GK & Shi W 2014 featureCounts: an efficient general purpose program for
675   assigning sequence reads to genomic features. *Bioinformatics (Oxford, England)* **30**
676   923–930. (doi:10.1093/bioinformatics/btt656)

677   Madeddu P, Anania V, Alagna S, Troffa C, Parpaglia PP, Tonolo G, Demontis MP, Varoni MV,
678   Fattaccio C & Glorioso N 1992 Role of brain kallikrein-kinin system in regulation of
679   adrenocorticotropin release. *The American Journal of Physiology* **262** E312-318.
680   (doi:10.1152/ajpendo.1992.262.3.E312)

681   Mallet C, Féraud O, Ouengue-Mbélé G, Gaillard I, Sappay N, Vittet D & Vilgrain I 2003
682   Differential expression of VEGF receptors in adrenal atrophy induced by
683   dexamethasone: a protective role of ACTH. *American Journal of Physiology-*
684   *Endocrinology and Metabolism* **284** E156–E167. (doi:10.1152/ajpendo.00450.2001)

685   Matthews SG & McGowan PO 2019 Developmental programming of the HPA axis and
686   related behaviours: epigenetic mechanisms. *Journal of Endocrinology* **242** T69–T79.
687   (doi:10.1530/JOE-19-0057)

688   Mayran A, Sochodolsky K, Khetchoumian K, Harris J, Gauthier Y, Bemmo A, Balsalobre A &
689   Drouin J 2019 Pioneer and nonpioneer factor cooperation drives lineage specific
690   chromatin opening. *Nature Communications* **10** 1–13. (doi:10.1038/s41467-019-
691   11791-9)

692   McDowell IC, Barrera A, D'Ippolito AM, Vockley CM, Hong LK, Leichter SM, Bartelt LC,
693   Majoros WH, Song L, Safi A *et al.* 2018 Glucocorticoid receptor recruits to enhancers
694   and drives activation by motif-directed binding. *Genome Research* **28** 1272–1284.
695   (doi:10.1101/gr.233346.117)

696   Mi H, Muruganujan A, Ebert D, Huang X & Thomas PD 2019 PANTHER version 14: more
697   genomes, a new PANTHER GO-slim and improvements in enrichment analysis tools.
698   *Nucleic Acids Research* **47** D419–D426. (doi:10.1093/nar/gky1038)

699   Newson MJF, Roberts EM, Pope GR, Lolait SJ & O'Carroll A-M 2009 The effects of apelin on
700   hypothalamic–pituitary–adrenal axis neuroendocrine function are mediated through

701   corticotrophin-releasing factor- and vasopressin-dependent mechanisms. *The*
702   *Journal of Endocrinology* **202** 123–129. (doi:10.1677/JOE-09-0093)

703 Nicholson S, Campbell E, Torrellas A, Beckford U, Altaher R, Sandford R, Scraggs R, Gillham B
704   & Jones M 1984 Recovery of the hypothalamo-pituitary-adrenocortical axis in the rat
705   after long-term dexamethasone treatment. *Neuroendocrinology* **39** 343–349.
706   (doi:10.1159/000124002)

707 Nixon M, Mackenzie SD, Taylor AI, Homer NZM, Livingstone DE, Mouras R, Morgan RA, Mole
708   DJ, Stimson RH, Reynolds RM *et al.* 2016 ABCC1 confers tissue-specific sensitivity to
709   cortisol versus corticosterone: A rationale for safer glucocorticoid replacement
710   therapy. *Science Translational Medicine* **8** 352ra109-352ra109.
711   (doi:10.1126/scitranslmed.aaf9074)

712 Ostrander MM, Ulrich-Lai YM, Choi DC, Richtand NM & Herman JP 2006 Hypoactivity of the
713   Hypothalamo-Pituitary-Adrenocortical Axis during Recovery from Chronic Variable
714   Stress. *Endocrinology* **147** 2008–2017. (doi:10.1210/en.2005-1041)

715 Pinto S, Roseberry AG, Liu H, Diano S, Shanabrough M, Cai X, Friedman JM & Horvath TL
716   2004 Rapid rewiring of arcuate nucleus feeding circuits by leptin. *Science (New York,*
717   *N.Y.)* **304** 110–115. (doi:10.1126/science.1089459)

718 Ruggiero C & Lalli E 2016 Impact of ACTH Signaling on Transcriptional Regulation of
719   Steroidogenic Genes. *Frontiers in Endocrinology* **7**. (doi:10.3389/fendo.2016.00024)

720 Schinkel AH, Wagenaar E, Deemter L van, Mol CA & Borst P 1995 Absence of the mdr1a P-
721   Glycoprotein in mice affects tissue distribution and pharmacokinetics of
722   dexamethasone, digoxin, and cyclosporin A. *The Journal of Clinical Investigation* **96**
723   1698–1705. (doi:10.1172/JCI118214)

724 Schlaghecke R, Kornely E, Santen RT & Ridderskamp P 1992 The effect of long-term
725   glucocorticoid therapy on pituitary-adrenal responses to exogenous corticotropin-
726   releasing hormone. *The New England Journal of Medicine* **326** 226–230.
727   (doi:10.1056/NEJM199201233260403)

728 Schuetz P, Christ-Crain M, Schild U, Süess E, Facompre M, Baty F, Nusbaumer C, Brutsche M
729   & Müller B 2008 Effect of a 14-day course of systemic corticosteroids on the
730   hypothalamic-pituitary-adrenal-axis in patients with acute exacerbation of chronic
731   obstructive pulmonary disease. *BMC Pulmonary Medicine* **8** 1. (doi:10.1186/1471-
732   2466-8-1)

733 Schürmeyer TH, Tsokos GC, Avgerinos PC, Balow JE, D'agata R, Loriaux DL & Chrousos GP
734   1985 Pituitary-Adrenal Responsiveness to Corticotropin-Releasing Hormone in
735   Patients Receiving Chronic, Alternate Day Glucocorticoid Therapy. *The Journal of*
736   *Clinical Endocrinology & Metabolism* **61** 22–27. (doi:10.1210/jcem-61-1-22)

737 Spiga F, Zhao Z & Lightman SL 2020 Prolonged treatment with the synthetic glucocorticoid
738   methylprednisolone affects adrenal steroidogenic function and response to

739   inflammatory stress in the rat. *Brain, Behavior, and Immunity*.
740   (doi:10.1016/j.bbi.2020.03.001)

741 Steenblock C, Celis MFR de, Silva LFD, Pawolski V, Brennand A, Werdermann M, Berger I,
742   Santambrogio A, Peitzsch M, Andoniadou CL *et al.* 2018 Isolation and
743   characterization of adrenocortical progenitors involved in the adaptation to stress.
744   *Proceedings of the National Academy of Sciences* **115** 12997–13002.
745   (doi:10.1073/pnas.1814072115)

746 Verma M, Sooy K, Just G, Nixon M, Morgan R, Andrew R, Chapman KE & Homer NZM 2019
747   Quantitative analysis of 11-dehydrocorticosterone and corticosterone for preclinical
748   studies by liquid chromatography/triple quadrupole mass spectrometry. *Rapid
749   Communications in Mass Spectrometry* **n/a** e8610. (doi:10.1002/rcm.8610)

750 Yang N, Li T, Cheng J, Tuo Q & Shen J 2019 Role of apelin/APJ system in hypothalamic-
751   pituitary axis. *Clinica Chimica Acta* **499** 149–153. (doi:10.1016/j.cca.2019.09.011)

752

753

Acknowledgements

Figure legends

Figure 1. Schematic of experiments. A. Experiment 1. C57Bl6/J mice were assigned to receive DEX in drinking water (n = 6 mice in 3 cages) or water alone (n = 6 mice in 3 cages) for 4 weeks. Control mice received only standard drinking water (Group A). Following 4 weeks treatment, 2 animals selected at random from each cage were sacrificed (Group B). Following one further week, two further mice from each cage were collected as at time 0 (Group C). The last animals were collected 4 weeks after DEX withdrawal (Group D). Age matched controls were assigned to group A. **B. Experiment 2.** Here, 16 cages of 3 mice were randomly assigned to 4 treatment groups, A; receiving water in drinking water for 8 weeks, B; drinking water for 4 weeks and then DEX for 4 weeks, C; water for 3 weeks, DEX for 4 weeks then 1 week with drinking water and D; DEX for 4 weeks then drinking water for 4 weeks. All animals were collected at a single time point at the end of the experiment as above. Animals were reverse lit and collected at the point of waking. **C. Experiment 3** was conducted as experiment 2, except that animals were not reverse lit and *Pomc*-eGFP mice were used. 12 cages of 3 animals were assigned randomly to the four groups. At the end of the experiment, tissue was collected as experiment 1 and 2, but anterior pituitary was dissected and dissociated for FACS isolation of corticotrophs. RNA from isolated corticotrophs underwent RNA-seq. Numbers to the right refer to numbers of animals/ in how many cages.

Figure 2. Dexamethasone reduces weight and corticosterone production that persists 1 week following treatment withdrawal. A and B. Adrenal weight DEX treatment did not significantly affect adrenal weight. The mean weight of both adrenal glands at collection is presented with box and whisker charts from experiment 2 (A) and experiment 1 (B). **C and D. Adrenal weight/bodyweight D and E.** The adrenal weights as a proportion of bodyweight are presented for experiment 2(C) and experiment 2 (D). **E and F. Corticosterone levels.** DEX treatment reduced corticosterone levels that were still reduced 1 week after stopping DEX treatment at waking (pm) (experiment 2) (E), but which had returned to normal basal levels (am; rest period) (experiment 1) (F). Corticosterone levels had returned to the level of controls 4 weeks after stopping DEX treatment. **G and H 11-dehydrocorticosterone levels.** As E and F but measured 11-dehydrocorticosterone. **I. ACTH levels.** Plasma ACTH was not significantly affected by DEX treatment. One week after stopping DEX, there was greater variation in ACTH levels. Data from experiment 2. The dotted box highlights mice with recovered ACTH production, the dashed box shows mice with unrecovered ACTH production; grey circles in this box are mice with Corticosterone levels below controls, blue circles are mice with corticosterone within the range of controls. **J. Relationship between plasma corticosterone and ACTH.** DEX treatment (yellow triangles) reduced both plasma ACTH and corticosterone compared to controls (grey circles). One week after stopping DEX (blue squares), there was greater variation between animals with some showing high ACTH levels but lower corticosterone (dotted box) and some showing inappropriate ACTH levels for the lower corticosterone levels (dashed box). Four weeks after stopping DEX, ACTH and corticosterone levels had returned to level of controls (green crosses). Data from experiment 2. **Legend.** Grey dots and boxes represent control mice (Group A), yellow those who have had 4 weeks of DEX treatment (Group B), blue those one week after withdrawal of DEX (Group C) and green those 4 weeks after treatment withdrawal (Group D). Data analysed by linear mixed model with group as dependent variable and cage as

809   random factor. Tukey-adjusted post hoc tests compared to control group are
810   indicated above boxes where significant differences were identified. *** p<0.001, **
811   p<0.01, * p<0.05.

812   **Figure 3. DEX treatment induces significant and persistent changes in adrenal**
813   **gene expression. A. Hypothalamus.** DEX treatment did not affect gene expression
814   of *Avp, Crh, Nr3C1*, or *Nr3c2* in whole hypothalamus (data from experiment 1). **B**
815   **and C. Adrenal.** Dex reduced the adrenal expression of the ACTH receptor (*Mc2r*),
816   steroidogenic enzymes (*Cyp11a1 Hsd3b2* and *Star*) and increased expression of the
817   glucocorticoid receptor (*Nr3c1*) and Mineralocorticoid receptor (*Nr3c2*). Data are
818   shown from experiment 1 (am panels) and experiment 2 (pm panels). For ease of
819   comparison, control samples from each time point in experiment 1 have been
820   combined, ddCt values were made in comparison to time-matched adrenal glands.
821   **Legend.** Grey bars represent control mice (Group A), yellow those who have had 4
822   weeks of DEX treatment (Group B), blue those one week after withdrawal of DEX
823   (Group C), and green those 4 weeks after treatment withdrawal (Group D). Data
824   analysed by linear mixed model with group as dependent variable and cage as
825   random factor. Tukey-adjusted *post hoc* tests compared to control group are
826   indicated above bars (small asterixis) where significant differences were identified.
827   *** p<0.001, ** p<0.01, * p<0.05.

828   **Figure 4. DEX treatment significantly affects the corticotroph transcriptome**
829   **with changes evident 4 weeks following treatment withdrawal. A. eGFP**
830   **expression.** The eGFP expression of the isolated cells is shown. In groups A
831   (control; grey line) and C (1 week post DEX withdrawal; blue line) bimodal
832   populations of cells are apparent. The mean fluorescence of three sorts is shown
833   each comprising the dissociated pituitaries of 2-3 mice. **B. Heatmap showing**
834   **transcriptomic analysis of isolated cells.** The 60 genes with the most significant
835   difference between groups are shown. Relative expression across each row is
836   shown as per the colour code to the right of the panel. Columns indicate each
837   sample comprising cells isolated from 3 pituitaries and are clustered according to
838   gene expression pattern. Samples are clustered by Euclidean distance. **C. Selected**
839   **genes from RNA-seq from classes exhibiting persisting changes following**
840   **withdrawal of DEX.** Log2 fold change data are shown for genes that were
841   significantly affected by treatment and recovery along with the molecular function
842   class to which they belong (see table 1 and 2). Data are the same as those
843   presented in 4B. **Legend.** Grey lines/bars represent control mice (Group A); yellow
844   those who have had 4 weeks of DEX treatment (Group B); blue those one week after
845   withdrawal of DEX (Group C); and green those 4 weeks after treatment withdrawal
846   (Group D).

847

848

849   **Table 1. 151 differentially expressed genes and the time points at which they**
850   **were up- or down-regulated.** Genes were clustered into 27 subsets based upon
851   their expression relative to controls in each treatment group. Vs. Group B and Group
852   C in rows and Group D in columns. Very few genes demonstrate persistent change
853   in expression in the same direction over all three time points.

Table 2. Over-representation test for classes of genes with significant differential expression in experiment 3. Genes with differential expression were assessed for over-enrichment using PANTHER version 15.0, GO-slim molecular function. Binomial test with Bonferroni correction was applied to compare the list of differentially expressed genes with that expected.

Table 3. Over-representation test for classes of genes with changes across three groups with direction of change in expression. Genes with differential expression were assessed for over-enrichment using PANTHER version 15.0, GO-slim molecular function. Binomial test with Bonferroni correction was applied to compare the list of differentially expressed genes with that expected. Data are shown from classes identified in more than one comparison.
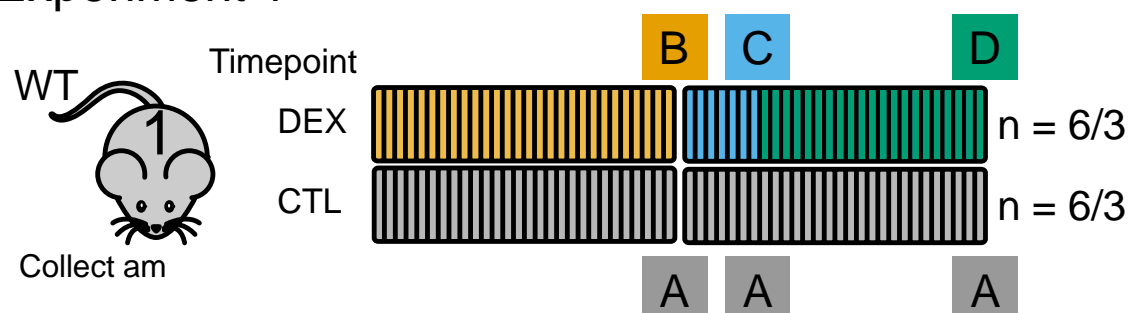
Figure S1. A. A. Bodyweight. DEX treat inhibited weight gain but this returned to control levels 4 weeks after stopping treatment. The weight of each mouse in experiment 2 is shown as representative. Mice were weighed twice a week. Mean and 95% confidence intervals are presented as lines. N = 16 cages of 3 mice. ### p<0.0001 for interaction between weight and time assessed by linear mixed model with cage and individual as random factor to account for repeated measures. Coloured bars at the bottom of the figure indicate time when mice were exposed to DEX. **B. Adrenal weight** weights of adrenals from experiment 3 were not significantly affected by treatment but were reduced and remained lower 4 weeks after stopping DEX. **C. Dexamethasone levels**. Plasma dexamethasone was measured at the end of the rest period (experiment 2). DEX increased measured DEX, which were undetectable in control groups or following 1 week of withdrawal of DEX. **D. Comparison of RNA-seq and qPCR from whole pituitary.** qPCR of whole pituitary and 6 key genes for corticotroph function is shown in the top panel. Pituitaries were collected in experiment 1 (n = 5-6 from 3 cages). Data analysed by linear mixed model with group as dependent variable and cage as random factor. Tukey-adjusted post hoc tests compared to control group are indicated above bars (small asterixis) where significant differences were identified. *** p<0.001, ** p<0.01, * p<0.05. The bottom panel shows for comparison the relative cpm to Group A (control) from the RNA-seq (experiment 3) (n = 3 pools of 2-3 pituitaries). *** p<0.0001; FDR. **Legend.** Grey dots and boxes represent control mice (Group A), yellow those who have had 4 weeks of DEX treatment (Group B), blue those one week after withdrawal of DEX (Group C), and green those 4 weeks after treatment withdrawal (Group D). Data analysed by linear mixed model with group as dependent variable and cage as random factor.

Figure S2. A. Fluorescence of isolated cells from each sort. FACS GFP distribution is shown for each sort of 2-3 anterior pituitaries following treatment (experiment 3). **B.** Raw counts of Pax7 and Pcsk2, markers of melanotrophs for comparison with panel A. Expression of melanotroph specific genes does not associate with sorts with larger secondary peaks of higher fluorescence. **C.** Number of cells, percent of fluorescent cells, and number of reads obtained form each sample from dissociated anterior pituitaries obtained in experiment 3. There were no significant difference between groups. N = 3 pools of 2-3 pituitaries. **Legend.** Grey dots and boxes represent control mice (Group A), yellow those who have had 4 weeks of DEX treatment (Group B), blue those one week after withdrawal of DEX (Group C), and green those 4 weeks after treatment withdrawal (Group D).
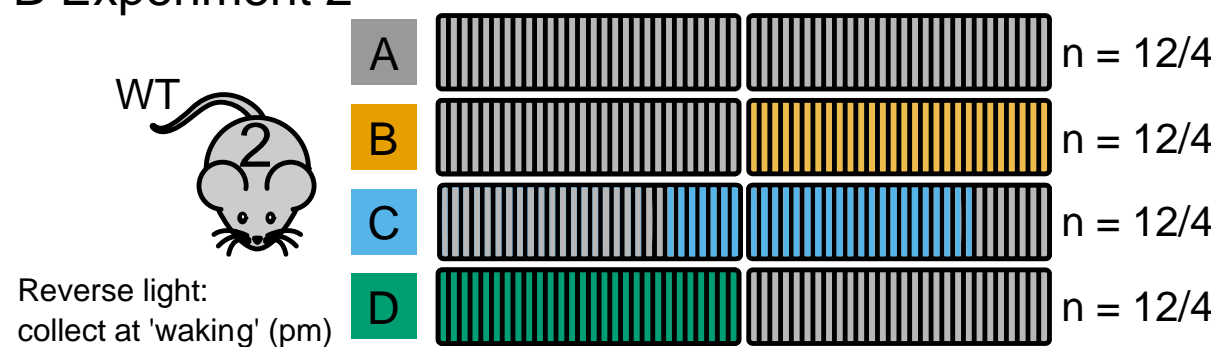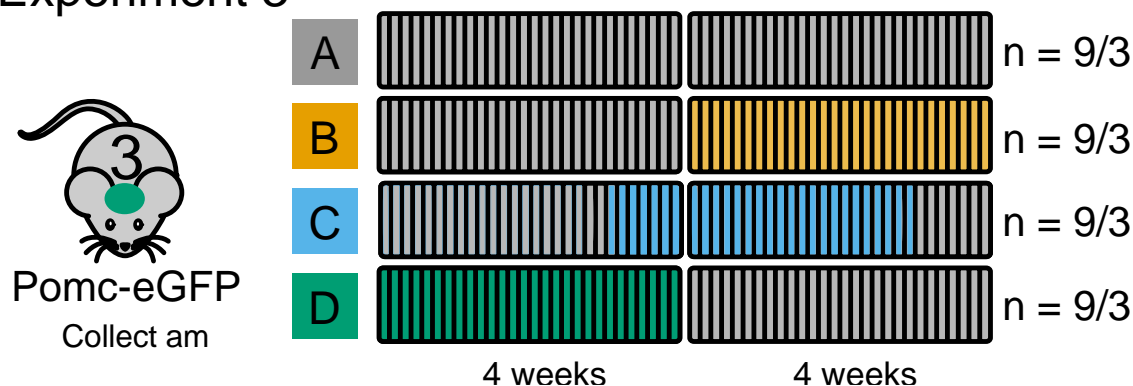
902 **Figures**

903 **Figure 1**

A Experiment 1

B Experiment 2
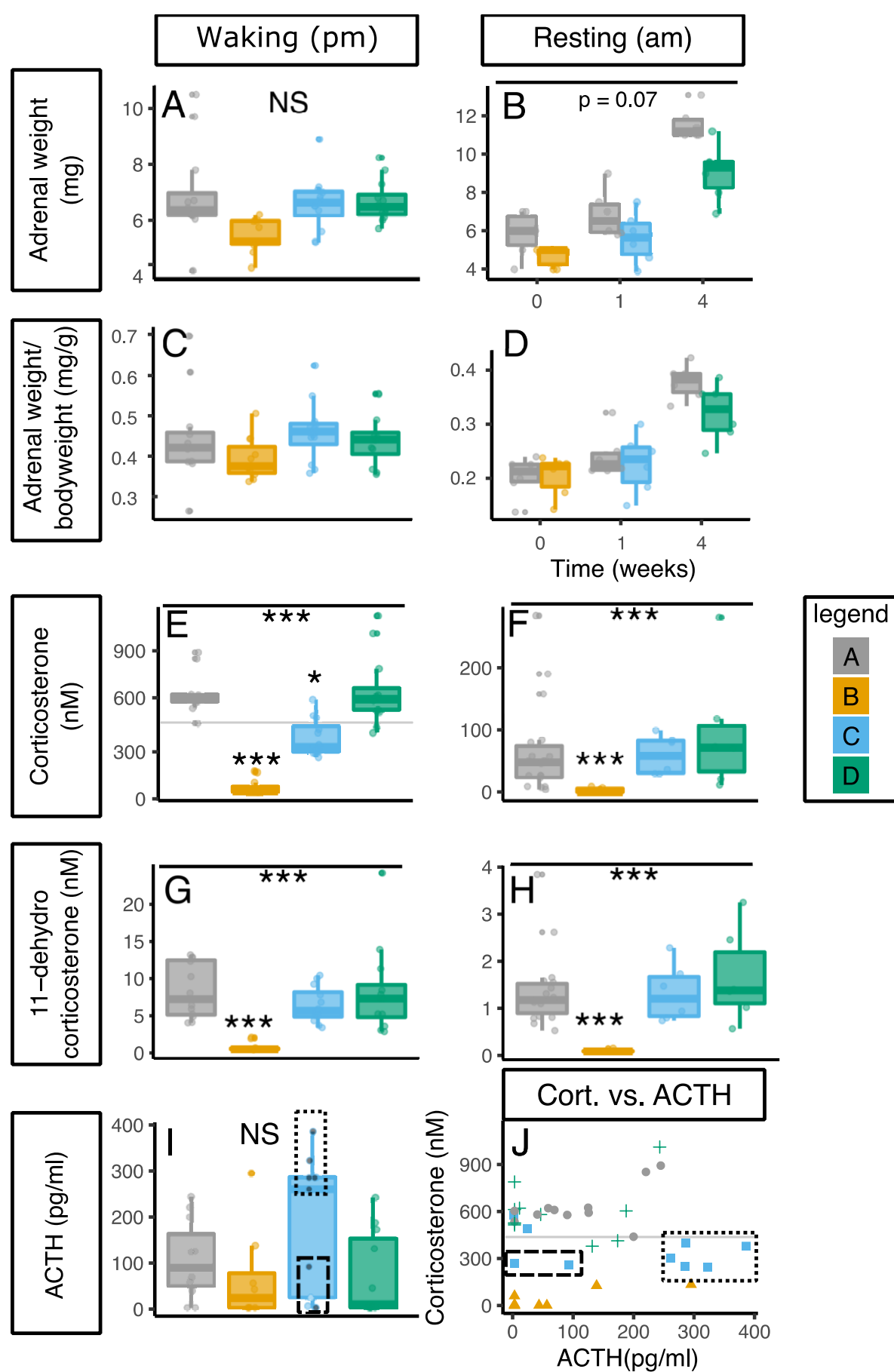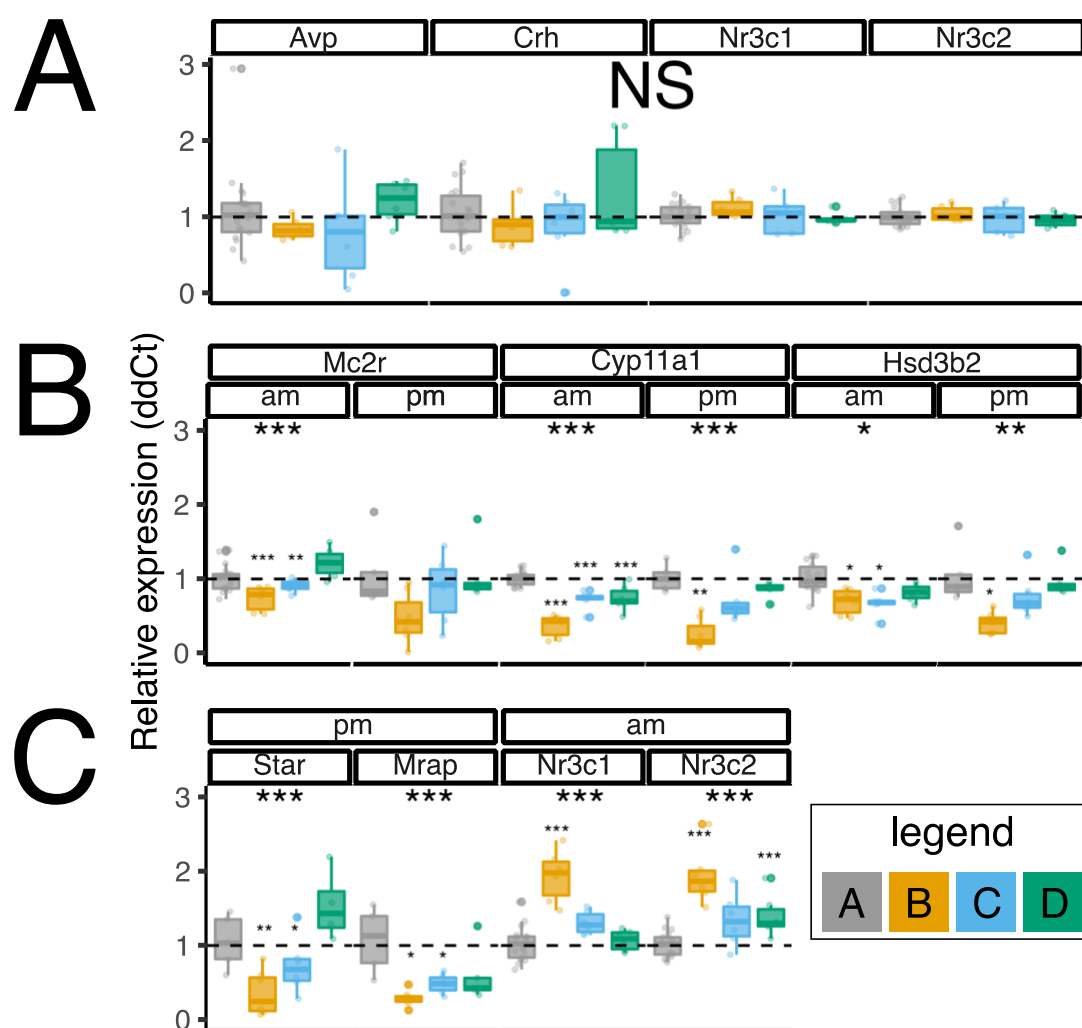
C Experiment 3

904
905
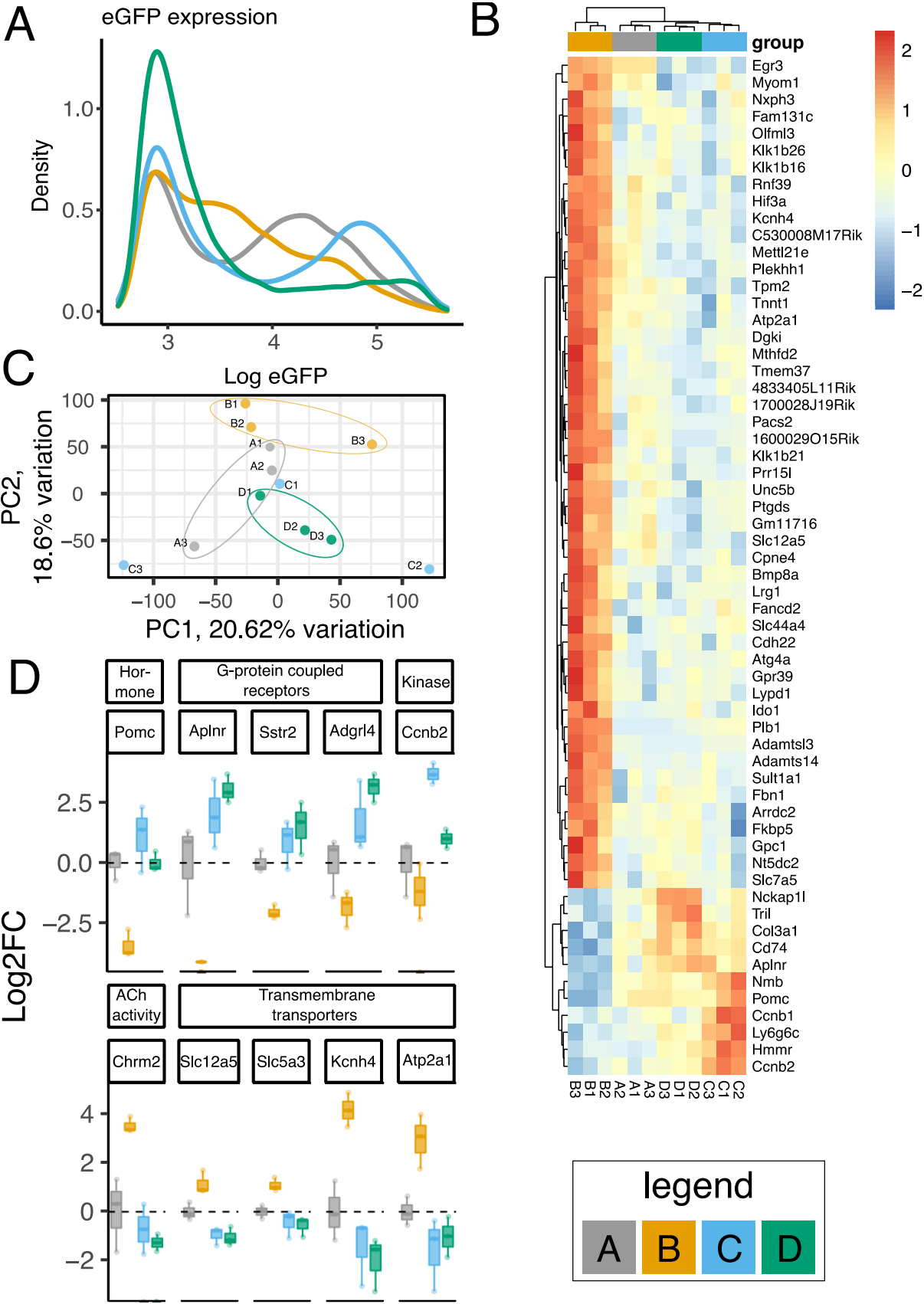
906 **Figure 2**

907

908 **Figure 3**

911 **Figure 4**

912
913

914 **Table 1**

Table 1

B\D	up	ns	down	D/C
	group 1 Plb1, Krt19	**group 7** Adamts14, Fancd2, Klk1b4	**group 3**	up
up	Fbn1, Ido1, Penk, Klk1b24, Oaf, Col8a2	Ptgds, Klk1b21, Tmem37, Dgki, Klk1b26, 4833405L11Rik, Cdh22, Sult1a1, Pacs2, Gpc1, Olfml3, Nt5dc2, Prr15l, Atg4a, Gpr39, Lypd1, Arrdc2, Tnnt1, Klk1b16, Lrg1, C530008M17Rik, Slc44a4, Cpne4, Slc7a5, Fkbp5, Mthfd2, Unc5b, Gpr1, 1700028J19Rik, Fam131c, Pik3ip1, Ttyh1, Ccnb1, Usp54, Plekhh1, Ciart, E230001N04Rik, Ankmy1, Glb1l2, Nxph3, Aatk, Cobl, Smoc2, Ankdd1b, Mindy4b-ps, Frmd4a, Sez6l, Atp7b, Gm38619, Lrrc75b, Sipa1l1, Angptl7, Gm27252, Sec14l4, Platr25, Unc5a, Slc5a3, Cab39l, Mapt, Ptprv, Wdr93, Rabep2, Fstl3, Prss57, Slc27a3, Susd4, 2410002F23Rik, Slc24a4, Mrps6, Frmpd1	Adamtsl3, Mettl21e, Bmp8a, Slc12a5, Myom1, Gm11716, Klk1b5, Myh11, Dgkk, Asic2, Pkd1l2, Gm38304	ns
		Atp2a1, Map3k6, Cntfr, Otog	Kcnh4, Hif3a, Tpm2, Rnf39, 1600029O15Rik, Chrm2	down
	group 5 Hmmr, Col4a1, Anln, Col4a2	**group 8** Ttyh1, Ccnb1	**group 6**	up
ns	Tril, Cpxm2, H6pd, Prelp, F2r, Fbln5, Plat, Nid2, Mlc1	Tmem145, Srpk1, Zbtb16, Cxcl12, Rptor		ns
	Inhbb		Egr3	down
	group 4 Ly6g6c, Aplnr, Pbk, Top2a, Adgrl4, Il16, Plbd1, Kdr, Pdgfrb, Sstr2, Rrm2, H2-Q6, Itgal, Pecam1	**group 9** Nmb, Ccnb2, Pomc	**group 2** Igha	up
down	Col3a1, Cd74, Nckap1l, H2-Aa, H2-DMb1, H2-Eb1, H2-Ab1, Mfap4	Psmb8, Rtn4rl1		ns

915

916 **Table 2**

917

PANTHER GO-Slim Molecular Function	Mus musculus - REFLIST	Number of genes (154)	Number of expected genes	Over or under represtation	A vs B t (fold Enrichment)	(P-value)	
transporter activity (GO:0005215)	782	10	5.41	+	1.85	0.05	Atp7b Slc7a5 Ttyh1 Slc24a4 Atp2a1 Slc12a5 Slc27a3 Pkd1l2 Slc5a3 Kcnh4
ion transmembrane transporter activity (GO:0015075)	581	9	4.02	+	2.24	0.02	Atp7b Slc7a5 Ttyh1 Slc24a4 Atp2a1 Slc12a5 Pkd1l2 Slc5a3 Kcnh4
inorganic molecular entity transmembrane transporter activity (GO:0015318)	550	9	3.8	+	2.37	0.01	Atp7b Slc7a5 Ttyh1 Slc24a4 Atp2a1 Slc12a5 Pkd1l2 Slc5a3 Kcnh4
kinase activity (GO:0016301)	572	8	3.96	+	2.02	0.05	Srpk1 Ccnb2 Dgki Dhkk Ccnb1 Pdgfrb Cab39l Map3k6
phosphotransferase activity, alcohol group as acceptor (GO:0016773)	534	8	3.69	+	2.17	0.03	Srpk1 Ccnb2 Dgki Dgkk Ccnb1 Pdgfrb Cab39l Map3k6
metal ion transmembrane transporter activity (GO:0046873)	310	7	2.14	+	3.26	0.01	Atp7b Slc24a4 Atp2a1 Slc12a5 Pkd1l2 Slc12a5 Kcnh4
cation transmembrane transporter activity (GO:0008324)	424	7	2.93	+	2.39	0.03	Atp7b Slc24a4 Atp2a1 Slc12a5 Pkd1l2 Slc5a3 Kcnh4
inorganic cation transmembrane transporter activity (GO:0022890)	395	7	2.73	+	2.56	0.02	Atp7b Slc24a4 Atp2a1 Slc12a5 Pkd1l2 Slc5a3 Kcnh4
active transmembrane transporter activity (GO:0022804)	218	5	1.51	+	3.32	0.02	Atp7b Slc24a4 Atp2a1 Slc12a5 Slc5a3

receptor regulator activity (GO:0030545)	255	5	1.76	+	2.83	0.03	Lypd1 Il16 Inhbb Bmp8a Dkk3
monovalent inorganic cation transmembrane transporter activity (GO:0015077)	261	5	1.81	+	2.77	0.04	Slc24a4 Atp2a1 Slc12a5 Slc5a3 Kcnh4
active ion transmembrane transporter activity (GO:0022853)	156	5	1.08	+	4.63	0.00	Atp7b Slc24a4 Atp2a1 Slc12a5 Slc5a3
organic cyclic compound binding (GO:0097159)	1680	4	11.62	-	0.34	0.01	Chrm Ciart Mrps6 Gata2
kinase binding (GO:0019900)	158	4	1.09	+	3.66	0.02	Ccnb2 Nell2 Myom1 Ccnb1
heterocyclic compound binding (GO:1901363)	1638	4	11.33	-	0.35	0.01	Chrm2 Ciart Mrps6 Gata2
calcium ion transmembrane transporter activity (GO:0015085)	84	3	0.58	+	5.16	0.02	Slc24a4 Atp2a1 Pkd1l2
cytokine activity (GO:0005125)	116	3	0.8	+	3.74	0.05	Il16 Inhbb Bmp8a
nucleic acid binding (GO:0003676)	1293	3	8.94	-	0.34	0.02	Ciart Mrps6 Gata2
carboxypeptidase activity (GO:0004180)	30	2	0.21	+	9.64	0.02	Cpxm2 Mindy4b-ps
postsynaptic neurotransmitter receptor activity (GO:0098960)	49	2	0.34	+	5.9	0.05	Chrm2 Lypd1
growth factor binding (GO:0019838)	38	2	0.26	+	7.61	0.03	Gpc1
glycosaminoglycan binding (GO:0005539)	42	2	0.29	+	6.88	0.03	Nell2 Rtn4rl1
acetylcholine receptor activity (GO:0015464)	28	2	0.19	+	10.33	0.02	Chrm2 Lypd1
cyclin-dependent protein serine/threonine kinase regulator activity (GO:0016538)	35	2	0.24	+	8.26	0.02	Ccnb1 Ccnb2
acetylcholine binding (GO:0042166)	28	2	0.19	+	10.33	0.02	Chrm2 Lypd1
neuropeptide binding (GO:0042923)	21	2	0.15	+	13.77	0.01	Sstr1 Gpr1
heparin binding (GO:0008201)	27	2	0.19	+	10.71	0.02	Nell2 Rtn4rl1
fibroblast growth factor binding (GO:0017134)	6	1	0.04	+	24.1	0.04	Gpc1
lipopolysaccharide binding (GO:0001530)	7	1	0.05	+	20.65	0.05	Tril

918

919 **Table 3**

| Molecular function	Mus Mus genes	Enriched	Expected	Fold enrichment	Significance	A vs B	A vs C	A vs D	Genes
G protein-coupled receptor activity (GO:0004930)	405	3	0.56	5.32	1.87E-02	Down	Up	Up	Aplnr; Sstr2; Adgrl4
neuropeptide binding (GO:0042923)	21	1	0.03	34.2	3.02E-02	Down	Up	Up	Sstr2
peptide binding (GO:0042277)	179	2	0.25	8.02	2.61E-02	Down	Up	Up	Sstr2; Aplnr
amide binding (GO:0033218)	194	2	0.27	7.4	3.03E-02	Down	Up		Aplnr; Sstr2
cyclin-dependent protein serine/threonine kinase regulator activity (GO:0016538)	35	1	0.05	20.52	4.89E-02	Down	Up		CCnb2
molecular transducer activity (GO:0060089)	1349	5	1.88	2.66	3.73E-02	Down	Up		Aplnr; Pdgfrb; Ccnb2; Sstr2; Adgrl4
Rac GTPase binding (GO:0048365)	26	1	0.04	27.62	3.69E-02	Down		Up	Nck1l
acetylcholine binding (GO:0042166)	28	2	0.12	17.1	6.90E-03	Up	Down	Down	Lypd1; Chrm2
acetylcholine receptor activity (GO:0015464)	28	2	0.12	17.1	6.90E-03	Up	Down	Down	Lypd1; Chrm2
actin filament binding (GO:0051015)	84	2	0.35	5.7	4.99E-02	Up	Down	Down	Myom1; Tpm2
cation transmembrane transporter activity (GO:0008324)	424	7	1.77	3.95	2.15E-03	Up	Down	Down	Slc12a5; Slc5a3; Atp7b; Slc24a4; Kcnh4; Atp2a1; Pkd1l2
hormone binding (GO:0042562)	52	2	0.22	9.21	2.13E-02	Up	Down	Down	Lypd1; Chrm2
inorganic cation transmembrane transporter activity (GO:0022890)	395	7	1.65	4.24	1.45E-03	Up	Down	Down	Slc12a5; Slc5a3; Atp7b; Slc24a4; Kcnh4; Atp2a1; Pkd1l2
inorganic molecular entity transmembrane transporter activity (GO:0015318)	550	8	2.3	3.48	2.28E-03	Up	Down	Down	Slc12a5; Slc5a3; Atp7b; Slc24a4; Kcnh4;

									Slc7a5; Atp2a1; Pkd1l2
ion transmembrane transporter activity (GO:0015075)	581	8	2.43	3.3	3.17E-03	Up	Down	Down	Slc12a5; Slc5a3; Atp7b; Slc24a4; Kcnh4; Slc7a5; Atp2a1; Pkd1l2
metal ion transmembrane transporter activity (GO:0046873)	310	7	1.29	5.41	3.60E-04	Up	Down	Down	Slc12a5; Slc5a3; Atp7b; Slc24a4; Kcnh4; Atp2a1; Pkd1l2
monovalent inorganic cation transmembrane transporter activity (GO:0015077)	261	5	1.09	4.59	5.10E-03	Up	Down	Down	Scl12a5; Slc5a3; Kcnh4; Atp2a1
postsynaptic neurotransmitter receptor activity (GO:0098960)	49	2	0.2	9.77	1.91E-02	Up	Down	Down	Lypd1; Chrm2
transmembrane transporter activity (GO:0022857)	701	8	2.93	2.73	9.41E-03	Up	Down	Down	Slc12a5; Slc5a3; Atp7b; Slc24a4; Kcnh4; Slc7a5; Atp2a1; Pkd1l2
ammonium ion binding (GO:0070405)	80	2	0.33	5.99	4.59E-02	Up	Down		Lypd1; Chrm2
calcium ion transmembrane transporter activity (GO:0015085)	84	3	0.35	8.55	5.74E-03	Up	Down		Slc24a4; Atp2a1; Pkd1l2
potassium ion transmembrane transporter activity (GO:0015079)	139	3	0.58	5.17	2.15E-02	Up		Down	Slc12a5; Kcnh4
transporter activity (GO:0005215)	782	9	3.27	2.76	5.65E-03	Up		Down	Slc12a5; Kcnh4; Pkd1l2
extracellular matrix structural constituent (GO:0005201)	11	1	0.05	21.76	4.88E-02	Up		Up	Fbn1
oxidoreductase activity, acting on single donors with incorporation of molecular oxygen, incorporation of two atoms of oxygen (GO:0016702)	10	1	0.04	23.94	4.48E-02	Up		Up	Ido1
DNA-binding transcription factor	618	2	0.31	6.55	3.60E-02		Down	Down	Hif3a; Egr3

activity (GO:0003700)									

920

921 **Figure S1**

922
923
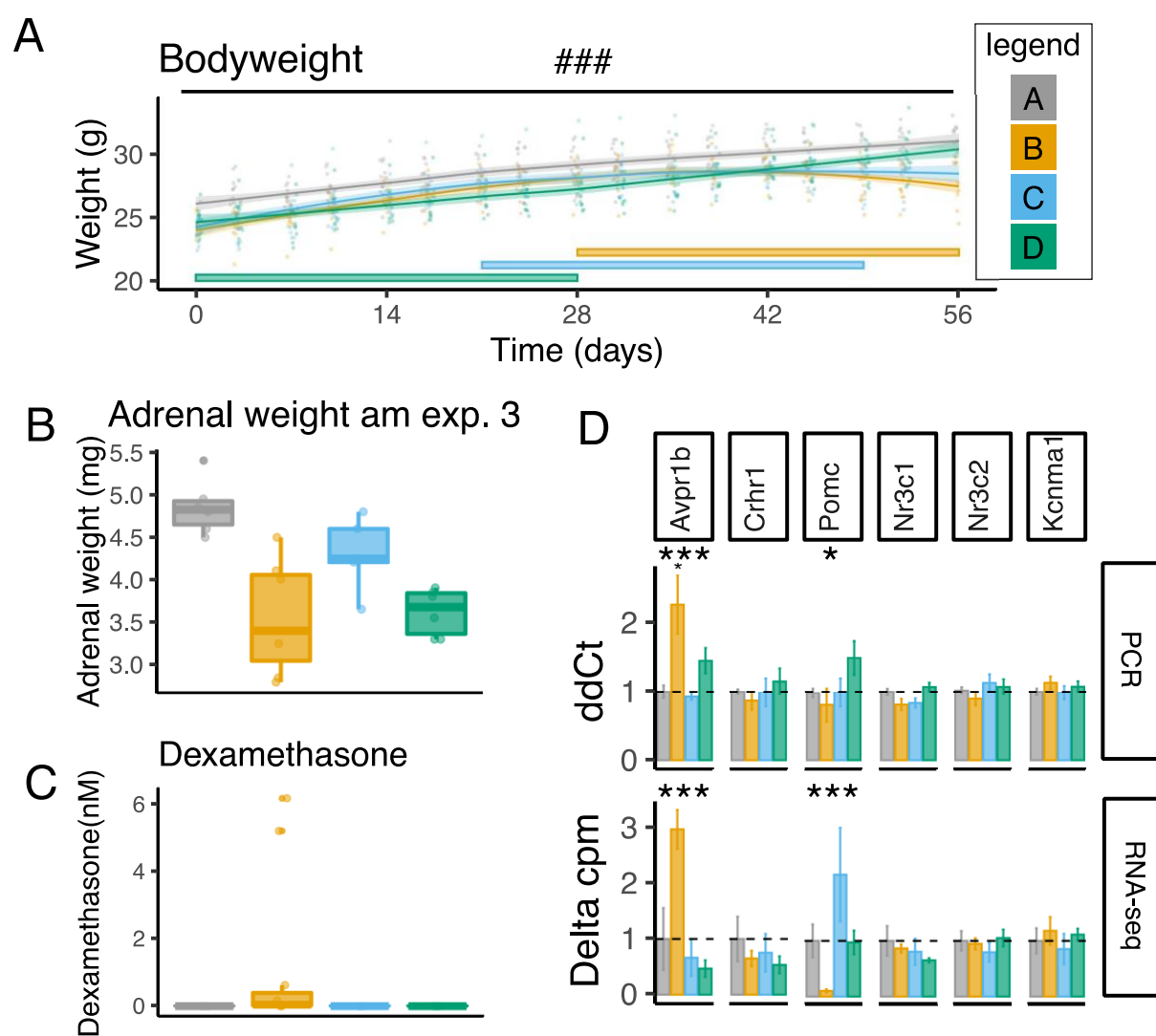
924 **Figure S2**
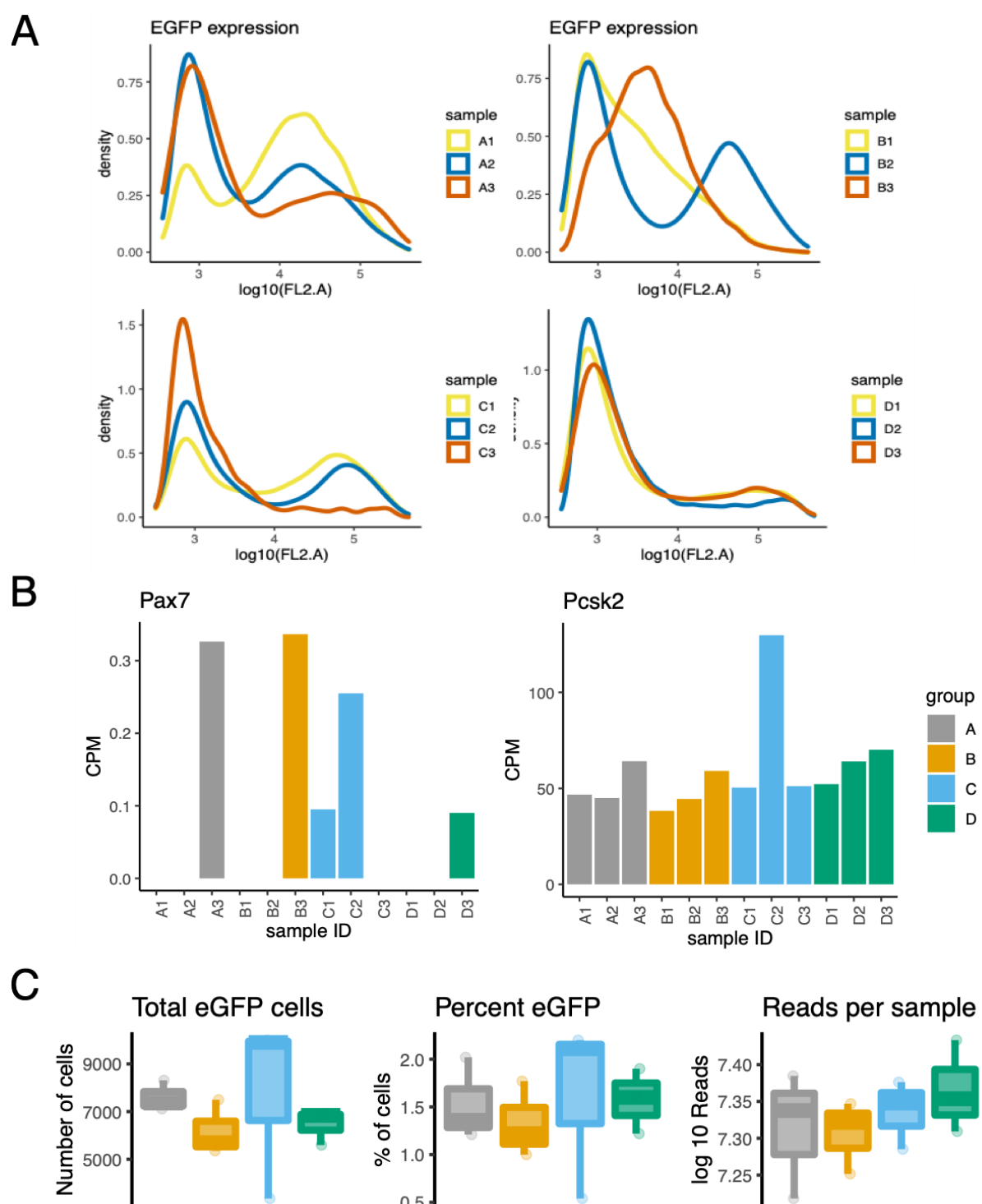
928 SUPPLEMENTAL TABLE 1: Gene ontology analysis of GC induced genes
929 (Molecular function)

Enrichment FDR	Genes in list	Total genes	Functional Category	Genes
0.000	7	135	Hydrolase activity, acting on carbon-nitrogen (but not peptide) bonds	MTHFD2 KLK1B16 KLK1B26 KLK1B24 KLK1B5 KLK1B4 KLK1B21
0.000	6	83	Hydrolase activity, acting on carbon-nitrogen (but not peptide) bonds, in linear amides	KLK1B16 KLK1B26 KLK1B24 KLK1B5 KLK1B4 KLK1B21
0.001	7	198	Serine-type endopeptidase activity	KLK1B5 PRSS57 KLK1B16 KLK1B26 KLK1B24 KLK1B4 KLK1B21
0.002	7	217	Serine-type peptidase activity	KLK1B5 PRSS57 KLK1B16 KLK1B26 KLK1B24 KLK1B4 KLK1B21
0.002	7	222	Serine hydrolase activity	KLK1B5 PRSS57 KLK1B16 KLK1B26 KLK1B24 KLK1B4 KLK1B21
0.003	3	23	Structural constituent of muscle	MYOM1 MYH11 KRT19
0.004	9	469	Endopeptidase activity	ATG4A KLK1B5 PRSS57 KLK1B16 KLK1B26 ADAMTS14 KLK1B24 KLK1B4 KLK1B21
0.004	11	683	Peptidase activity	ATG4A KLK1B26 ADAMTS14 KLK1B5 KLK1B21 PRSS57 USP54 KLK1B16 KLK1B24 KLK1B4 ADAMTSL3
0.006	2	7	Netrin receptor activity	UNC5B UNC5A
0.009	8	427	Metal ion transmembrane transporter activity	ATP7B SLC12A5 ATP2A1 KCNH4 SLC24A4 SLC5A3 ASIC2 TMEM37
0.009	10	654	Peptidase activity, acting on L-amino acid peptides	ATG4A KLK1B5 PRSS57 USP54 KLK1B16 KLK1B26 ADAMTS14 KLK1B24 KLK1B4 KLK1B21
0.014	2	12	Diacylglycerol kinase activity	DGKI DGKK
0.020	9	622	Cation transmembrane transporter activity	ATP7B SLC12A5 ATP2A1 KCNH4 SLC24A4 SLC5A3 SLC44A4 ASIC2 TMEM37
0.030	2	19	NAD+ kinase activity	DGKI DGKK
0.038	8	574	Inorganic cation transmembrane transporter activity	ATP7B SLC12A5 ATP2A1 KCNH4 SLC24A4 SLC5A3 ASIC2 TMEM37
0.040	10	851	Ion transmembrane transporter activity	ATP7B SLC12A5 ATP2A1 KCNH4 SLC7A5 SLC24A4 SLC5A3 SLC44A4 ASIC2 TMEM37
0.045	6	362	Monovalent inorganic cation transmembrane transporter activity	SLC12A5 ATP2A1 KCNH4 SLC24A4 SLC5A3 ASIC2

930
931

932 SUPPLEMENTAL TABLE 2: Gene ontology analysis of GC suppressed genes
933 (Molecular function)

Enrichment FDR	Genes in list	Total genes	Functional Category	Genes
0.001	3	51	Antigen binding	H2-Q6 H2-AA H2-AB1
0.001	5	291	Peptide binding	SSTR2 H2-Q6 H2-AA H2-AB1 CD74
0.001	3	33	Peptide antigen binding	H2-Q6 H2-AA H2-AB1
0.001	2	7	CD4 receptor binding	IL16 CD74
0.001	5	358	Amide binding	SSTR2 H2-Q6 H2-AA H2-AB1 CD74
0.001	2	12	Platelet-derived growth factor binding	PDGFRB COL3A1
0.002	8	1443	Protein dimerization activity	RRM2 PECAM1 TOP2A ITGAL ADGRL4 H2-AA H2-Q6 H2-AB1
0.005	8	1628	Signaling receptor binding	POMC H2-Q6 IL16 CD74 PDGFRB COL3A1 KDR NMB
0.005	3	144	Growth factor binding	PDGFRB COL3A1 KDR
0.005	5	607	Protein heterodimerization activity	TOP2A ITGAL H2-AA H2-Q6 H2-AB1
0.005	2	34	Neuropeptide receptor binding	POMC NMB
0.013	3	223	Cell adhesion molecule binding	COL3A1 ITGAL KDR
0.014	2	68	Transmembrane receptor protein tyrosine kinase activity	PDGFRB KDR
0.014	6	1207	Protein-containing complex binding	NCKAP1L CD74 COL3A1 ITGAL KDR H2-Q6
0.020	2	85	Transmembrane receptor protein kinase activity	PDGFRB KDR
0.023	8	2327	Enzyme binding	NCKAP1L CCNB2 TOP2A PDGFRB COL3A1 CD74 H2-AB1 PECAM1
0.026	4	633	Protein kinase activity	CCNB2 PBK PDGFRB KDR
0.029	8	2473	Signaling receptor activity	ADGRL4 APLNR SSTR2 CD74 PDGFRB ITGAL RTN4RL1 KDR
0.030	2	118	Integrin binding	COL3A1 KDR
0.030	8	2521	Molecular transducer activity	ADGRL4 APLNR SSTR2 CD74 PDGFRB ITGAL RTN4RL1 KDR
0.031	2	128	Extracellular matrix structural constituent	COL3A1 MFAP4
0.032	2	136	Protein tyrosine kinase activity	PDGFRB KDR
0.032	4	735	Phosphotransferase activity, alcohol group as acceptor	CCNB2 PBK PDGFRB KDR
0.032	2	140	G protein-coupled peptide receptor activity	APLNR SSTR2
0.035	2	149	Peptide receptor activity	APLNR SSTR2
0.039	2	162	Protein kinase regulator activity	CCNB2 NCKAP1L
0.043	4	840	Kinase activity	CCNB2 PBK PDGFRB KDR
0.044	7	2304	Transmembrane signaling receptor activity	ADGRL4 APLNR SSTR2 CD74 PDGFRB ITGAL KDR
0.050	2	194	Kinase regulator activity	CCNB2 NCKAP1L

934